

Performance Analysis of the Matrix Pair Beamformer with Matrix Mismatch

Jianshu Chen, *Student Member, IEEE*, Jian Wang, Xiu-Ming Shan,
Ning Ge, *Member, IEEE* and Xiang-Gen Xia, *Fellow, IEEE*

EDICS: SAM-PERF

Abstract

Matrix pair beamformer (MPB) is a blind beamformer. It exploits the temporal structure of the signal of interest (SOI) and applies generalized eigen-decomposition to a covariance matrix pair. Unlike other blind algorithms, it only uses the second order statistics. A key assumption in the previous work is that the two matrices have the same interference statistics. However, this assumption may be invalid in the presence of multipath propagations or certain “smart” jammers, and we call it as matrix mismatch. This paper analyzes the performance of MPB with matrix mismatch. First, we propose a general framework that covers the existing schemes. Then, we derive its normalized output SINR. It reveals that the matrix mismatch leads to a threshold effect caused by “steering vector competition”. Second, using matrix perturbation theory, we find that, if there are generalized eigenvalues that are infinite, the threshold will increase unboundedly with the interference power. This is highly probable when there are multiple periodical interferers. Finally, we present simulation results to verify our analysis.

Index Terms

This work was supported by the National Natural Science Foundation of China under contract No. 60972019 and No. 60928001. Jianshu Chen was with the Department of Electronic Engineering, Tsinghua University, Beijing, P. R. China, 100084. He is with the Department of Electrical Engineering, University of California, Los Angeles, CA 90095, USA. (e-mail: jshchen@ee.ucla.edu)

Jian Wang, Xiu-Ming Shan and Ning Ge are with the Department of Electronic Engineering, Tsinghua University, Beijing, P. R. China, 100084. (e-mail: {jian-wang, shanxm, gening} @tsinghua.edu.cn)

Xiang-Gen Xia is with the Department of Electrical and Computer Engineering, University of Delaware, Newark, DE 19716, USA. (e-mail: xxia@ee.udel.edu). His work was supported in part by the Air Force Office of Scientific Research (AFOSR) under Grant No. FA9550-08-1-0219, the National Science Foundation (NSF) under Grant CCF-0964500, and the World Class University (WCU) Program 2008-000-20014-0, National Research Foundation, Korea.

I. INTRODUCTION

Beamforming is a spatial filter, which combines the outputs of multiple sensor elements by an appropriately designed weight vector so as to pass a signal of interest (SOI) while rejecting interfering signals. Since the pioneering work of Howells [1], Applebaum [2] and Widrow [3], it has been intensively studied during the past decades and widely applied in radar, sonar and wireless communications [3]–[11] etc. For a comprehensive review, we refer to [12]–[15] and the references therein.

There are various forms of implementations for a beamformer. Some use the direction of arrival (DOA) of the SOI and directly calculate the weight vector by sample matrix inversion (SMI) [16]. Some employ a reference signal (e.g. training signal [17] and decision feedback signal [6]) to iteratively calculate the weight vector. And there are also blind beamformers which do not require the DOA or the reference signal [18]–[31].

To achieve blind beamforming, we need to exploit the special properties of the SOI, such as constant modulus, non-Gaussianness, high order statistics etc. One important property is the temporal structure of the SOI. Such kind of blind beamformers are extensively studied for CDMA systems, where the inherent structure of the spreading codes can be exploited [23]–[26], [28]–[31]. The advantage of this scheme is that it only relies on the second order statistics of the covariance matrix pair. Although the implementation details differ, the main idea of these approaches is to exploit a pair of array covariance matrix and hence will be referred to as matrix pair beamformer (MPB) in this paper. The MPB projects the discrete sequence in each antenna onto the space spanned by the SOI's signature vector (for a CDMA system, it is the spreading code vector) and another carefully designed base vector. Then two sets of array snapshots (i.e. signal snapshot and interference snapshot) are acquired to calculate a pair of covariance matrices. With the processing gain, the desired signal power in the signal snapshot is generally greater than that in the interference snapshot. *A key and common assumption is that the interference statistics in the two snapshots are identical.* These two features enable the separation of the signal steering vector and the interference covariance matrix from the two matrices. And the weight vector derived from the dominant eigenvector of the matrix pair will maximize the output signal to interference plus noise ratio (SINR).

However, this key assumption that the two matrices share the same interference statistics is not valid in many cases, which we refer to as *matrix mismatch*. Matrix mismatch may occur when there are interferers

with certain periodical structure, such as multiple access interference (MAI) in CDMA systems, tones and some other “smart jammers” in radar systems and it may lead to the failure of a system. In practical applications, to avoid such an unexpected failure, it is necessary to understand the detailed performance of a scheme when the assumption/condition is not satisfied. To our best knowledge, little effort has been devoted to analyzing the effect of matrix mismatch on the performance of MPB. This paper aims to analyze the MPB’s performance under matrix mismatch, and our contributions are:

- proposing a general framework to model various existing MPB schemes;
- deriving analytical expressions for the normalized output SINR as the performance measure;
- discovering a threshold effect for MPB, i.e., due to matrix mismatch, the performance of MPB degrades rapidly when the input signal to noise ratio (SNR) is below a predicted threshold, and the main beam points to the directions of the interferers;
- explaining how MPB works “blindly” by “steering vector competition”;
- discussing various factors that have impact on the threshold, and showing that when there is an generalized eigenvalue that is infinite which is called *the noise-free covariance matrix pair*, the threshold SNR increases unboundedly with the interference power;
- discussing several typical scenarios and showing that MPB is very vulnerable to multiple periodical interferers.

The rest of the paper is organized as follows. Sec. II presents a general framework of MPB to cover and reinterpret the basic ideas in [23]–[31], followed by a formulation of the matrix mismatch problem. In Sec. III, we present the expressions for MPB’s weight vector and its normalized output SINR, which uncovers the inherent threshold effect caused by matrix mismatch. The discussion relies heavily on the approximation of the generalized eigenvalue, which is derived in Appendix A using Gerschgorin theorem [32], [33]. Sec. IV applies the Weyl-Lidskii type theorem in matrix perturbation theory [32] to analyze MPB’s threshold SNR, and discusses it in two typical scenarios. Finally, Sec. V presents simulation results to verify our theoretical analysis and Sec. VI concludes the whole paper.

II. PROBLEM FORMULATION

A. Signal Model

Consider an antenna array of L isotropic elements that receives $D + 1$ signals from a far field. After preprocessing (e.g. mixing, filtering, etc.) and sampling, the output $L \times 1$ array vector can be written as

$$\mathbf{x}(n) = \sum_{i=0}^D \sqrt{P_i} s_i(n) \mathbf{a}_i + \mathbf{v}(n), \quad (1)$$

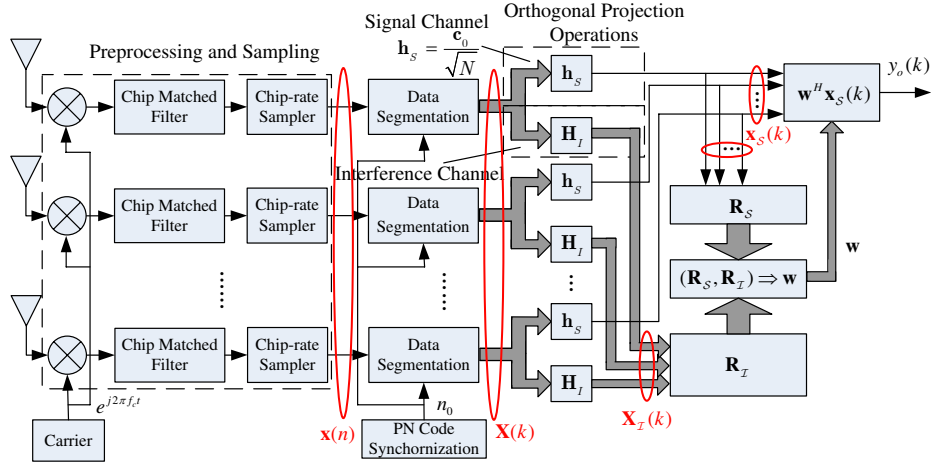


Fig. 1. Block diagram of the matrix pair beamformer in a CDMA system. Data corresponding to the k symbol are blocked and projected onto two spaces to produce signal channel snapshot $\mathbf{x}_S(k)$ and interference channel snapshot $\mathbf{X}_I(k)$, respectively.

where $s_i(n)$ is the discrete sequence of the i th signal with normalized power; P_i is its power; \mathbf{a}_i is the steering vector, which depends on the DOA and the array geometry; $\mathbf{v}(n)$ is the additive white Gaussian noise (AWGN) vector with zero mean and covariance matrix $\sigma^2 \mathbf{I}$. Assume $s_0(n)$ is the SOI, and $s_1(n), s_2(n), \dots, s_D(n)$ model all the possible interferers like MAI and jammer etc. This paper considers the case when $s_0(n)$ has some inherent temporal structure expressed as

$$s_0(n) = \sum_{k=-\infty}^{+\infty} b_0(k) c_0[n - \tau(k)], \quad (2)$$

where $c_0(n)$ is known and supported on $0 \leq n \leq N - 1$. Thus, $s_0(n)$ can be viewed as a train of pulses, with each of them being a delayed and scaled replica of $c_0(n)$. And $\tau(k)$ and $b_0(k)$ are the corresponding delay and amplitude of the k th pulse. This model is common in modern communication systems. For instance, in CDMA system, $c_0(n)$ is the spreading code of the desired user, $b_0(k)$ is its data bits and $\tau(k)$ is the delay of the k th symbol. Without loss of generality, let us consider $b_0(k) \in \{\pm 1\}$, $c_0(n) \in \{\pm 1\}$ and $\tau(k) = kN + n_0$. Then N is the processing gain and n_0 is the propagation delay.

B. A General Framework of the Matrix Pair Beamformer

We first propose a framework called *matrix pair beamformer* (MPB) to cover the common ideas in [23]–[31]. Our strategy is to use orthogonal projection operation to model their ways of estimating the covariance matrix pair. By this framework, we will find a common threshold effect in these methods.

The steering vector \mathbf{a}_i in (1) is a spatial signature of the i th signal, which is different from other \mathbf{a}_j so long as they arrive from different directions. Beamformer is a spatial filter that exploits such difference to pass the desired signal $s_0(n)$ while suppressing $s_1(n) \dots s_D(n)$ and $\mathbf{v}(n)$. A statistically optimum beamformer [12], [15] generally requires at least, either explicitly or implicitly, the information about the steering vector \mathbf{a}_0 and the interference covariance matrix. The latter one may be replaced by the data covariance matrix, so the remaining problem is how to acquire \mathbf{a}_0 . In DOA-based beamformer, it is calculated by the DOA and array manifold information. As for training-based method or decision directed method, it is inherent in the correlation vector between the reference signal and the data vector.

To work “blindly”, i.e. without any explicit information of DOA, the methods in [23]–[31] exploit the SOI’s temporal signature $c_0(n)$ to acquire these spatial statistical information. Specifically, it is implemented by two orthogonal projections and a generalized eigen-decomposition of a covariance matrix pair. Hence, we refer to them as matrix pair beamformer (MPB) in this literature. In Fig. 1, we summarize the common structure of MPB. With the data segmentation, the array outputs corresponding to the k th symbol of the desired user can be expressed in the following matrix form:

$$\mathbf{X}(k) \triangleq \begin{bmatrix} \mathbf{x}(kN + n_0) & \cdots & \mathbf{x}(kN + n_0 + N - 1) \end{bmatrix} = \left[\sqrt{P_0} b_0(k) \right] \mathbf{a}_0 \mathbf{c}_0^T + \underbrace{\mathbf{A}_I \Theta_I^{\frac{1}{2}} \mathbf{S}_I^T(k) + \mathbf{V}(k)}_{\mathbf{Z}(k)} \quad (3)$$

where

$$\begin{aligned} \mathbf{A}_I &\triangleq \begin{bmatrix} \mathbf{a}_1 & \mathbf{a}_2 & \cdots & \mathbf{a}_D \end{bmatrix} \\ \mathbf{c}_0 &\triangleq \begin{bmatrix} c_0(0) & c_0(1) & \cdots & c_0(N-1) \end{bmatrix}^T \\ \mathbf{S}_I(k) &\triangleq \begin{bmatrix} \mathbf{s}_1(k) & \mathbf{s}_2(k) & \cdots & \mathbf{s}_D(k) \end{bmatrix} \\ \mathbf{s}_i(k) &\triangleq \begin{bmatrix} s_i(kN + n_0) & \cdots & s_i(kN + n_0 + N - 1) \end{bmatrix}^T \\ \mathbf{V}(k) &\triangleq \begin{bmatrix} \mathbf{v}(kN + n_0) & \cdots & \mathbf{v}(kN + n_0 + N - 1) \end{bmatrix}. \\ \Theta_I &\triangleq \text{diag}\{P_1, P_2, \dots, P_D\}. \end{aligned}$$

Then, the k th data block in each antenna is projected onto two subspaces: signal space \mathcal{S} spanned by the SOI’s temporal signature vector $\mathbf{h}_S = \mathbf{c}_0 / \sqrt{N}$, and a specifically designed interference space $\mathcal{I} = \mathcal{R}\{\mathbf{H}_I\}$, respectively. Without loss of generality, assume the columns of $\mathbf{H}_I \in \mathbb{C}^{N \times r_I}$ are orthonormal. Then, the projections produce the signal snapshot $\mathbf{x}_S(k) = \mathbf{X}(k) \mathbf{h}_S^*$ and the interference snapshot $\mathbf{X}_I(k) = \mathbf{X}(k) \mathbf{H}_I^*$.

Define $\sigma_{S_0}^2 \triangleq NP_0$ and $\sigma_{I_0}^2 \triangleq \frac{P_0}{r_I} \|\mathbf{H}_I^H \mathbf{c}_0\|^2$. Then, the covariance matrices of $\mathbf{x}_S(k)$ and $\mathbf{X}_I(k)$ are

$$\mathbf{R}_S \triangleq \mathbf{E}\{\mathbf{x}_S(k)\mathbf{x}_S^H(k)\} = \sigma_{S_0}^2 \mathbf{a}_0 \mathbf{a}_0^H + \mathbf{Q}_S \quad (4)$$

$$\mathbf{R}_I \triangleq \frac{1}{r_I} \mathbf{E}\{\mathbf{X}_I(k)\mathbf{X}_I^H(k)\} = \sigma_{I_0}^2 \mathbf{a}_0 \mathbf{a}_0^H + \mathbf{Q}_I \quad (5)$$

where $\sigma_{S_0}^2$ and $\sigma_{I_0}^2$ are the SOI's powers in the *signal channel* and *interference channel* (c.f. Fig. 1), respectively. \mathbf{Q}_S and \mathbf{Q}_I are the covariance matrices of the interference-plus-noise in them, defined by

$$\mathbf{Q}_S = \mathbf{E}\{\mathbf{Z}(k)\mathbf{h}_S^* \mathbf{h}_S^T \mathbf{Z}^H(k)\} = \mathbf{A}_I \Phi_S \mathbf{A}_I^H + \sigma^2 \mathbf{I}, \quad (6)$$

$$\mathbf{Q}_I = \mathbf{E}\{\mathbf{Z}(k)\mathbf{H}_S^* \mathbf{H}_S^T \mathbf{Z}^H(k)\} = \mathbf{A}_I \Phi_I \mathbf{A}_I^H + \sigma^2 \mathbf{I}, \quad (7)$$

where $\Phi_S = \sigma^2 \text{INR} \cdot \Phi_{S_0}$, $\Phi_I = \sigma^2 \text{INR} \cdot \Phi_{I_0}$, $\text{INR} = P_1/\sigma^2$, and

$$\Phi_{S_0} = \Omega_I^{\frac{1}{2}} \mathbf{E}\{\mathbf{S}_I^T(k)\mathbf{h}_S^* \mathbf{h}_S^T \mathbf{S}_I^*(k)\} \Omega_I^{\frac{1}{2}}, \quad \Phi_{I_0} = \frac{1}{r_I} \Omega_I^{\frac{1}{2}} \mathbf{E}\{\mathbf{S}_I^T(k)\mathbf{H}_I^* \mathbf{H}_I^T \mathbf{S}_I^*(k)\} \Omega_I^{\frac{1}{2}}, \quad (8)$$

with $\Omega_I = (\Theta_I/\sigma^2)/\text{INR}$. We can see that Ω_I is independent of INR and only depends on the relative strength of the interferers. So are Φ_{S_0} and Φ_{I_0} , and we will use this conclusion in Sec. IV.

The MPB uses the eigenvector corresponding to the largest generalized eigenvalue of the matrix pair $(\mathbf{R}_S, \mathbf{R}_I)$ as the weight vector \mathbf{w} , which is the solution to the following equation

$$\mathbf{R}_S \mathbf{w} = \lambda_{\max} \mathbf{R}_I \mathbf{w}, \quad (9)$$

where λ_{\max} is the largest generalized eigenvalue of $(\mathbf{R}_S, \mathbf{R}_I)$. \mathbf{w} is applied to $\mathbf{x}_S(k)$ to yield the output

$$y_o(k) = \mathbf{w}^H \mathbf{x}_S(k) = \underbrace{[\sigma_{S_0} b_0(k)]}_{y_S(k)} \mathbf{w}^H \mathbf{a}_0 + \underbrace{\mathbf{w}^H \mathbf{Z}(k) \mathbf{h}_S^*}_{y_I(k)} \quad (10)$$

where $y_S(k)$ and $y_I(k)$ are the output signal and interference-plus-noise. Eq. (9) is also equivalent to

$$(\mathbf{R}_S - \mathbf{R}_I) \mathbf{w} = (\lambda_{\max} - 1) \mathbf{R}_I \mathbf{w}. \quad (11)$$

Using (4) and (5), we have

$$\mathbf{R}_S - \mathbf{R}_I = (\sigma_{S_0}^2 - \sigma_{I_0}^2) \mathbf{a}_0 \mathbf{a}_0^H + \mathbf{Q}_S - \mathbf{Q}_I. \quad (12)$$

Since the columns of \mathbf{H}_I are orthonormal, i.e. $\mathbf{H}_I^H \mathbf{H}_I = \mathbf{I}$, its spectral norm is one and we can have

$$\sigma_{I_0}^2 \triangleq \frac{P_0}{r_I} \|\mathbf{H}_I^H \mathbf{c}_0\|^2 \leq \frac{P_0}{r_I} \|\mathbf{H}_I\|^2 \|\mathbf{c}_0\|^2 = \frac{NP_0}{r_I} \leq \sigma_{S_0}^2.$$

The above inequality holds strictly when choosing $\mathbf{H}_I \neq \mathbf{h}_S$ (either $r_I > 1$ or $\mathbf{H}_I \neq \mathbf{h}_S$ for $r_I = 1$). Furthermore, it is commonly assumed [23]–[31] that $\mathbf{Q}_S = \mathbf{Q}_I$. Then, $\mathbf{Q}_S - \mathbf{Q}_I = \mathbf{O}$ in (12), and the dominant eigenvector of $(\mathbf{R}_S - \mathbf{R}_I, \mathbf{R}_I) = ((\sigma_{S_0}^2 - \sigma_{I_0}^2) \mathbf{a}_0 \mathbf{a}_0^H, \mathbf{R}_I)$ is

$$\mathbf{w}_{\text{opt}} = \mu \mathbf{R}_I^{-1} \mathbf{a}_0 = \mu' \mathbf{Q}_S^{-1} \mathbf{a}_0, \quad (13)$$

where μ and μ' are scalars. Then \mathbf{w}_{opt} will maximize the output interference plus noise ratio (SINR) [15], and the optimal SINR is

$$\text{SINR}_{\text{opt}} = \frac{\mathbb{E}\{|y_S(k)|^2\}}{\mathbb{E}\{|y_I(k)|^2\}} \Big|_{\mathbf{w}_{\text{opt}}} = \sigma_{S_0}^2 \mathbf{a}_0^H \mathbf{Q}_S^{-1} \mathbf{a}_0 \quad (14)$$

All the methods in [23]–[31] share the structures described above. They only differ in the dominant eigenvector searching algorithm and the interference space \mathcal{I} (i.e. $\mathbf{H}_{\mathcal{I}}$). In most existing approaches, \mathcal{I} is a one dimension space ($r_{\mathcal{I}} = 1$). The pre- and post-correlation (PAPC) scheme [23]–[27] uses $\mathbf{R}_{\mathcal{I}} = \mathbb{E}\{\mathbf{x}(n)\mathbf{x}^H(n)\}$, thus it is equivalent to choosing $\mathbf{H}_{\mathcal{I}}$ as

$$\mathbf{H}_{\mathcal{I}} = \begin{bmatrix} 0 & \cdots & 0 & 1 & 0 & \cdots & 0 \end{bmatrix}^T. \quad (15)$$

where only one component in $\mathbf{H}_{\mathcal{I}}$ is nonzero. The Maximin scheme in [28] and [29] employs a *monitor filter* to isolate the interference, which can be interpreted as

$$\mathbf{H}_{\mathcal{I}} = \mathbf{c}_0 \odot \begin{bmatrix} 1 & e^{j2\pi f_{\text{MF}}} & \cdots & e^{j2\pi f_{\text{MF}}(N-1)} \end{bmatrix}^T, \quad (16)$$

where $f_{\text{MF}} \in (0, 1]$ is the normalized center frequency of monitor filter, and \odot is the Hadamard product.

C. Matrix Mismatch

We see that the MPB relies heavily on the key assumption that $\mathbf{Q}_S = \mathbf{Q}_{\mathcal{I}}$, namely the interferers have the same second order statistics in the two channels. By (6)–(8), we know it is valid when each interferer is random enough in the temporal domain, say directional white noise (c.f. Sec. IV-B1). However, it is generally not satisfied, especially when there are multiple deterministic periodical interferers, like tones and MAI (c.f. Sec. IV-B2). This is because when the interferers are deterministic and periodical, the expectations in (8) can be eliminated. Then $\mathbf{Q}_S = \mathbf{Q}_{\mathcal{I}}$ requires $\mathbf{S}_I^T(k)\mathbf{h}_S^* = \mathbf{S}_I^T(k)\mathbf{H}_{\mathcal{I}}^*$, which is highly improbable when $\mathbf{h}_S \neq \mathbf{H}_{\mathcal{I}}$. We term this as “*matrix mismatch*”. To our best knowledge, very little effort has been devoted to analyze this problem. Therefore, we will investigate the performance of MPB in this more general case. Before we proceed, we define the normalized output SINR to measure performance degradation with respect to that of no matrix mismatch.

Definition 1: The *normalized output SINR* is defined as the actual output SINR of MPB normalized by the optimal value, i.e.

$$\mathbf{G} \triangleq \frac{\mathbb{E}\{|y_S(k)|^2\}}{\mathbb{E}\{|y_I(k)|^2\}} \Big|_{\mathbf{w}} \cdot \frac{1}{\text{SINR}_{\text{opt}}} \quad (17)$$

where SINR_{opt} is given by (14), and \mathbf{w} is the solution to (11) without the assumption of $\mathbf{Q}_S = \mathbf{Q}_{\mathcal{I}}$.

\mathbf{G} generally depends on the input SNR and the interference powers. So a reasonable way to characterize the performance is to plot \mathbf{G} against the input $\text{SNR} \triangleq \sigma_{S_0}^2/\sigma^2$, when fixing the interference powers. In the following sections, we will base our analysis on $\mathbf{G}(\text{SNR})$, which we will refer to as *operating curve*. Moreover, we assume infinite sample size so that the finite sample effect is ignored.

III. PERFORMANCE ANALYSIS OF THE MATRIX PAIR BEAMFORMER WITH MATRIX MISMATCH

In this section, we will derive the operating curve of MPB, and discuss how it works blindly.

A. Operating Curve of Matrix Pair Beamformer

We base our discussions on the following assumptions, and summarize the main result in theorem 1.

Assumption 1: The spacing of DOA between any two signals is large enough (greater than a mainlobe), so that $\{\mathbf{a}_i\}_{i=0}^D$ are linearly independent and the projection of \mathbf{a}_0 onto $\text{span}\{\mathbf{a}_i\}_{i=1}^D$ is much less than $\|\mathbf{a}_0\|$.

Assumption 2: The steering vectors of all signals are normalized so that $\|\mathbf{a}_i\|^2 = L$, ($i = 0, 1, \dots, D$).

Theorem 1 (operating curve): The normalized output SINR of MPB with matrix mismatch is

$$\mathbf{G}(\text{SNR}) = \begin{cases} \frac{P_I + 1}{P_I / [1 - \text{SNR}_{T0} / \text{SNR}]^2 + 1} G_U, & \text{SNR} > \text{SNR}_{T2} \\ \left[\frac{1 + K_0}{1 - \text{SNR} / \text{SNR}_{T0} + K_0 (L\beta \text{SNR} / N + 1)} \right]^2 G_L, & \text{SNR} < \text{SNR}_{T1} \end{cases} \quad (18)$$

where G_U and G_L are the normalized output SINR when $\text{SNR} = +\infty$ and $\text{SNR} = 0$ ($-\infty$ dB), respectively. $\beta \triangleq N\sigma_{I_0}^2/\sigma_{S_0}^2$ is the normalized power leakage ratio (PLR) in interference channel. $P_I \triangleq 1/G_U - 1$ is the output interference to noise ratio, and SNR_{T0} is the empirical threshold SNR. Their expressions are

$$G_U = \frac{\mathbf{a}_0^H \mathbf{Q}_I^{-1} \mathbf{a}_0}{\mathbf{a}_0^H \mathbf{Q}_S^{-1} \mathbf{a}_0} \cdot \frac{\mathbf{a}_0^H \mathbf{Q}_I^{-1} \mathbf{a}_0}{\mathbf{a}_0^H \mathbf{Q}_I^{-1} \mathbf{Q}_S \mathbf{Q}_I^{-1} \mathbf{a}_0} \quad (19)$$

$$\text{SNR}_{T0} = \frac{N}{L} \cdot \frac{1}{[(N - \beta)/(\gamma_1)^+ - \beta]^+} \quad (20)$$

$$K_0 = \frac{\beta + N/L / \text{SNR}_{T0}}{N - \beta} \left(\gamma_1 - \frac{N - \beta}{\beta} \right)^+ \quad (21)$$

where $(\cdot)^+ = \max\{\cdot, 0\}$, and γ_1 is the largest nonzero generalized eigenvalue of $(\mathbf{Q}_S - \mathbf{Q}_I, \mathbf{Q}_I)$.¹ The SNR at which $\mathbf{G}(\text{SNR})$ is close to G_L and G_U (within 3dB), which are given by

$$\text{SNR}_{T1} = \left(1 - \sqrt{\frac{1}{2}} \right) \text{SNR}_{T0}, \quad \text{SNR}_{T2} = \left(1 - \sqrt{\frac{P_I}{2P_I + 1}} \right)^{-1} \text{SNR}_{T0}, \quad (22)$$

¹If $(\mathbf{Q}_S - \mathbf{Q}_I, \mathbf{Q}_I)$ has less than D nonzero eigenvalues, pad them with zeros up to D and order them decreasingly.

respectively.

Though we will give expression for G_L in Sec. III-D, its specific values are of no interest to us. Fig. 2(a) shows a typical curve of $G(\text{SNR})$. We plot the curve in failure area and operating area given in (18), and connect their ends by a dashed line. We can see that the performance of beamformer degrades rapidly when the input SNR is below SNR_{T_2} . And it fails completely after reaching SNR_{T_1} . Therefore, matrix mismatch causes a threshold effect in MPB, and SNR_{T_2} is a critical parameter to be optimized.

There are two special cases of $G(\text{SNR})$. The first one is $\text{SNR}_{T_1}=\text{SNR}_{T_2}=0$ ($-\infty\text{dB}$). This happens when there is no matrix mismatch, i.e. $\mathbf{Q}_S=\mathbf{Q}_I$, so that $\gamma_1=0$ and SNR_{T_i} given by (20) and (22) are zero. Then, (18) implies the operating curve is a horizontal line as shown in Fig. 2(b). Another interesting case happens in PAPC schemes mentioned in II-B, whose PLR is $\beta=1>0$. If it further satisfies $(N-\beta)/\gamma_1<\beta$, then by (20) and (22), $\text{SNR}_{T_1}=\text{SNR}_{T_2} = +\infty$ and $G(\text{SNR})$ only has the failure area, which decreases in the order of $\mathcal{O}(\text{SNR}^{-2})$ (c.f. Fig. 2(c)). In the rest of the section, we will derive $G(\text{SNR})$ and reveal how MPB works blindly under matrix mismatch. The discussion of SNR_{T_0} is left to Sec. IV.

B. Derivation of the Weight Vector for MPB

As a step to prove Theorem 1, we first derive the expression of the weight vector for MPB. By the arguments in Sec. II-B, it is the solution to (11). Define $\Phi_\Delta \triangleq \Phi_S - \Phi_I$. Then, by (6), (7) and (12), the problem becomes solving the following generalized eigenequation

$$[(\sigma_{S_0}^2 - \sigma_{I_0}^2)\mathbf{a}_0\mathbf{a}_0^H + \mathbf{A}_I\Phi_\Delta\mathbf{A}_I^H]\mathbf{w} = (\lambda_{\max} - 1)\mathbf{R}_I\mathbf{w}, \quad (23)$$

where λ_{\max} is the largest eigenvalue of $(\mathbf{R}_S, \mathbf{R}_I)$. Sec. II-B already gave the result for \mathbf{w} when there is no matrix mismatch, i.e. $\Phi_\Delta=\mathbf{O}$ (or $\mathbf{Q}_S=\mathbf{Q}_I$). We concluded that it is optimal in the sense of maximizing the output SINR. However, in the presence of matrix mismatch, we have $\Phi_\Delta \neq \mathbf{O}$, which is the key challenge for solving (23). To deal with this problem, we first have the following two observations:

- By left-multiplying $\frac{1}{\lambda_{\max}-1}\mathbf{R}_I^{-1}$ to both sides of (23), we can see that \mathbf{w} can be expressed as

$$\mathbf{w} = \eta_0\mathbf{R}_I^{-1}\mathbf{a}_0 + \sum_{i=1}^D \eta_i\mathbf{R}_I^{-1}\mathbf{a}_i \quad (24)$$

i.e. it is a linear combination of $\mathbf{R}_I^{-1}\mathbf{a}_0, \mathbf{R}_I^{-1}\mathbf{a}_1, \dots, \mathbf{R}_I^{-1}\mathbf{a}_D$, where $\eta_0 = \frac{\sigma_{S_0}^2 - \sigma_{I_0}^2}{\lambda_{\max}-1}\mathbf{a}_0^H\mathbf{w}$, \mathbf{a}_i is the i th column of \mathbf{A}_I , and η_i is the i th component of $\boldsymbol{\eta} = \Phi_\Delta\mathbf{A}_I^H\mathbf{w}$. To determine $\eta_0, \eta_1, \dots, \eta_D$, we only need to substitute (24) back into (23) and solve a linear equation. However, we will immediately discover that the solution is intractable for further analysis because $\mathbf{A}_I^H\mathbf{R}_I^{-1}\mathbf{A}_I$ and Φ_Δ are not diagonal. To overcome this, we need the next observation.

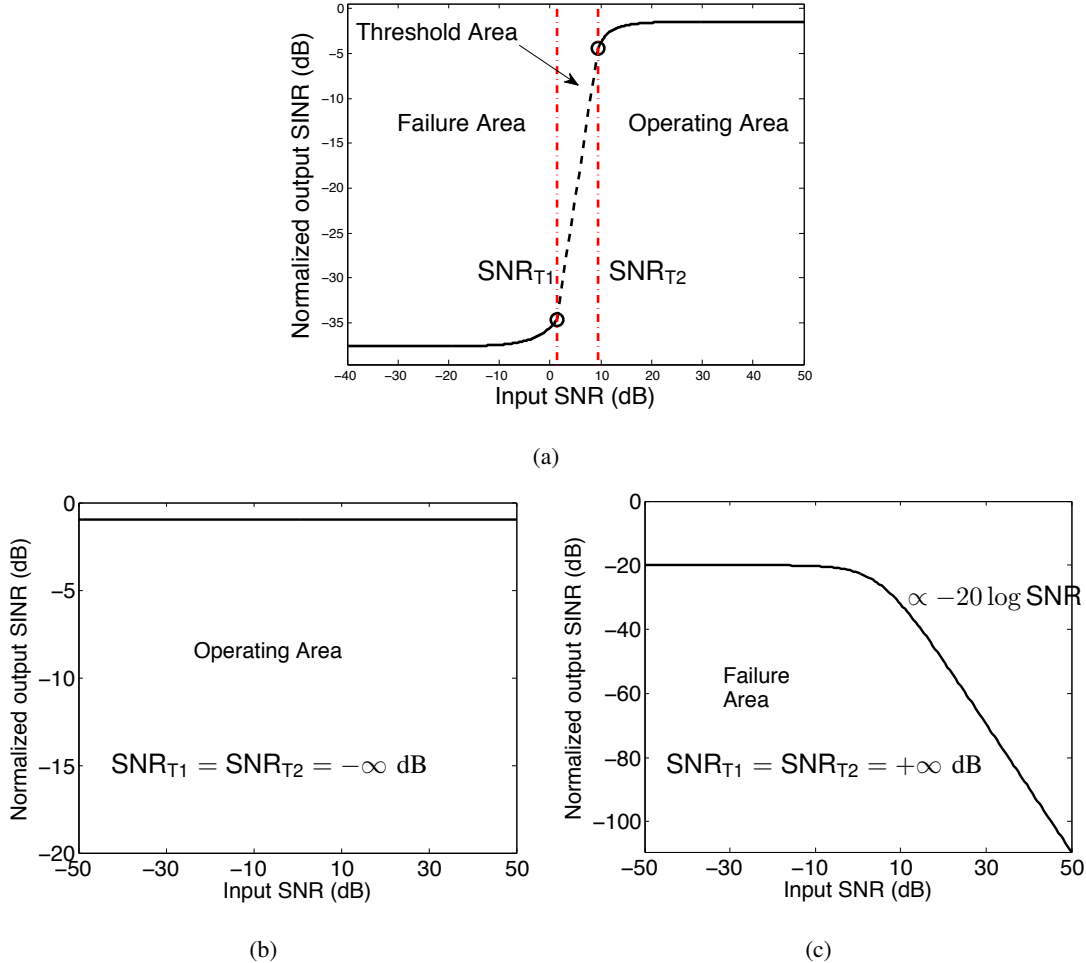


Fig. 2. (a) A typical curve of $G(\text{SNR})$ has failure area, threshold area and operating area, separated by SNR_{T1} and SNR_{T2} . (b) Without matrix mismatch, the curve has only operating area. (c) A curve has only failure area for some cases in PAPC.

- Suppose we can factorize Φ_{Δ} into diagonal form such that $\mathbf{A}_I \Phi_{\Delta} \mathbf{A}_I^H = \mathbf{A}_{\epsilon} \Gamma \mathbf{A}_{\epsilon}$ and $\mathbf{A}_{\epsilon}^H \mathbf{R}_{\mathcal{I}}^{-1} \mathbf{A}_{\epsilon} = \mathbf{I}$, where Γ is a diagonal matrix. Then, by repeating the above procedure except for replacing $\mathbf{a}_1, \dots, \mathbf{a}_D$ by $\mathbf{a}_{\epsilon_1}, \dots, \mathbf{a}_{\epsilon_D}$, with \mathbf{a}_{ϵ_i} being the i th column of \mathbf{A}_{ϵ} , we can solve \mathbf{w} as

$$\mathbf{w} = \eta_0 \left[\mathbf{R}_{\mathcal{I}}^{-1} \mathbf{a}_0 + \sum_{i=1}^D \frac{\gamma_i \tilde{\psi}_{T_i}}{\lambda_{\max} - 1 - \gamma_i} \mathbf{R}_{\mathcal{I}}^{-1} \mathbf{a}_{\epsilon_i} \right], \quad (25)$$

where γ_i is the i th diagonal component of Γ , η_0 is an arbitrary constant, and $\tilde{\psi}_{T_i} = \mathbf{a}_{\epsilon_i}^H \mathbf{R}_{\mathcal{I}}^{-1} \mathbf{a}_0$.

So far, the only thing left is to figure out a way to factorize Φ_{Δ} so that it meets the above requirement. Consider the generalized eigen-decomposition of the matrix pair $(\Phi_{\Delta}, (\mathbf{A}_I^H \mathbf{R}_{\mathcal{I}}^{-1} \mathbf{A}_I)^{-1})$. By the simultaneous diagonalization theorem (c.f. [34], pp.133), there exists a nonsingular matrix \mathbf{T} such that

$$\mathbf{T}^H \Phi_{\Delta} \mathbf{T} = \Gamma, \quad \mathbf{T}^H (\mathbf{A}_I^H \mathbf{R}_{\mathcal{I}}^{-1} \mathbf{A}_I)^{-1} \mathbf{T} = \mathbf{I}, \quad (26)$$

where $\mathbf{\Gamma} = \text{diag}(\gamma_1, \gamma_2, \dots, \gamma_D)$ is a diagonal matrix whose diagonal terms are the generalized eigenvalues of $(\mathbf{\Phi}_\Delta, (\mathbf{A}_I^H \mathbf{R}_T^{-1} \mathbf{A}_I)^{-1})$. Define $\mathbf{A}_\epsilon = \mathbf{A}_I (\mathbf{T}^{-1})^H$. Then, by (26), we can verify that

$$\mathbf{A}_I \mathbf{\Phi}_\Delta \mathbf{A}_I^H = \mathbf{A}_I (\mathbf{T}^{-1})^H \mathbf{\Gamma} \mathbf{T}^{-1} \mathbf{A}_I^H = \mathbf{A}_\epsilon \mathbf{\Gamma} \mathbf{A}_\epsilon^H$$

$$\mathbf{A}_\epsilon \mathbf{R}_T^{-1} \mathbf{A}_\epsilon = \mathbf{T}^{-1} \mathbf{A}_I^H \mathbf{R}_T^{-1} \mathbf{A}_I (\mathbf{T}^{-1})^H = \mathbf{I}.$$

Therefore, (26) is the exact decomposition of $\mathbf{\Phi}_\Delta$ we are looking for. Furthermore, by $\mathbf{A}_\epsilon = \mathbf{A}_I (\mathbf{T}^{-1})^H$, we notice that each column of \mathbf{A}_ϵ is in fact a linear combination of $\mathbf{a}_1, \dots, \mathbf{a}_D$. This, together with (25), implies that \mathbf{w} is still a linear combination of $\mathbf{R}_T^{-1} \mathbf{a}_0, \mathbf{R}_T^{-1} \mathbf{a}_1, \dots, \mathbf{R}_T^{-1} \mathbf{a}_D$, just as that in (24).

C. How MPB Works Blindly

To fully understand the behavior of MPB given by (25) and how it works blindly, we still need the expressions of λ_{\max} and γ_i . However, λ_{\max} and γ_i are the solutions to

$$\det \{ (\lambda - 1) \mathbf{R}_T - (\sigma_{S_0}^2 - \sigma_{T_0}^2) \mathbf{a}_0 \mathbf{a}_0^H - \mathbf{A}_I \mathbf{\Phi}_\Delta \mathbf{A}_I^H \} = 0 \quad (27)$$

$$\det \{ \lambda (\mathbf{A}_I^H \mathbf{R}_T^{-1} \mathbf{A}_I)^{-1} - \mathbf{\Phi}_\Delta \} = 0 \quad (28)$$

which are polynomial equations of degree $D + 1$ and D , respectively. It is known that there are no general closed-form solutions if their degrees are higher than four. Thus, our approach here is to derive approximate expressions for λ_{\max} and γ_i . The main idea is to transform (27) and (28) into eigenvalue problems of a diagonal matrix perturbed by a small term. Then we can approximate the eigenvalues by the diagonal entries, and bound the error using matrix perturbation theory.

We first discuss λ_{\max} . Before this, let's introduce the following identity which will be used repeatedly in the analysis and can be derived from Properties 16 and 17 in [34, pp.5].

$$\det(\lambda \mathbf{I} - \mathbf{X}\mathbf{Y}) = \lambda^{m-n} \cdot \det(\lambda \mathbf{I} - \mathbf{Y}\mathbf{X}) \quad (29)$$

where $\mathbf{X} \in \mathbb{C}^{m \times n}$ and $\mathbf{Y} \in \mathbb{C}^{n \times m}$. Substituting the factorization of $\mathbf{\Phi}_\Delta$ in (26) into (27) and using (29) as well as $\mathbf{A}_\epsilon = \mathbf{A}_I (\mathbf{T}^{-1})^H$, we can have the equivalent form of (27) as below

$$(\lambda - 1)^{L-D-1} \cdot \det \mathbf{R}_T \cdot \det \left\{ (\lambda - 1) \mathbf{I} - \begin{bmatrix} \sigma_{S_0}^2 - \sigma_{T_0}^2 & \mathbf{0}^T \\ \mathbf{0} & \mathbf{\Gamma} \end{bmatrix} \begin{bmatrix} \mathbf{a}_0^H \mathbf{R}_T^{-1} \mathbf{a}_0 & \mathbf{a}_0^H \mathbf{R}_T^{-1} \mathbf{A}_\epsilon \\ \mathbf{A}_\epsilon^H \mathbf{R}_T^{-1} \mathbf{a}_0 & \mathbf{A}_\epsilon^H \mathbf{R}_T^{-1} \mathbf{A}_\epsilon \end{bmatrix} \right\} = 0. \quad (30)$$

Then, (30) implies that the solution of (27) is the same as the eigenvalues of the following matrix

$$\mathbf{M} = \begin{bmatrix} \gamma_0 + 1 & \gamma_0 \sqrt{\frac{\sigma^2}{L}} \boldsymbol{\psi}_T^H \\ \frac{\sqrt{\frac{\sigma^2}{L}}}{\frac{L\beta}{N} \text{SNR} + 1} \mathbf{\Gamma} \boldsymbol{\psi}_T & \mathbf{\Gamma} + \mathbf{I} \end{bmatrix} \quad (31)$$

except for the multiplicity of ones, where we have used the second equality of (26). And γ_0 and ψ_T are

$$\gamma_0 \triangleq (\sigma_{S_0}^2 - \sigma_{I_0}^2) \mathbf{a}_0^H \mathbf{R}_T^{-1} \mathbf{a}_0, \quad \psi_T \triangleq \left(\frac{L\beta}{N} \text{SNR} + 1 \right) \mathbf{A}_\epsilon^H \mathbf{R}_T^{-1} \mathbf{a}_0 \quad (32)$$

Before proceeding on, we cite the following two lemmas. The first one is summarized from Lemma 1 and Lemma 2 in [35], and the second one can be found in [33, pp.344].

Lemma 1: The quantities $\mathbf{a}_0^H \mathbf{R}_T^{-1} \mathbf{a}_0$ and ψ_T have the following results

$$\mathbf{a}_0^H \mathbf{R}_T^{-1} \mathbf{a}_0 \approx \frac{L}{\sigma^2} \frac{N}{L\beta \text{SNR} + N}, \quad \|\psi_T\| \approx \sqrt{\frac{L}{\sigma^2} \kappa_0} \ll \sqrt{\frac{L}{\sigma^2}}.$$

where β is the PLR defined in Theorem 1, and κ_0 is a very small positive number independent of SNR.

Lemma 2 (Gerschgorin): Let matrix $\mathbf{A} \in \mathbb{C}^{n \times n}$ and a_{ij} be its i, j th element. Define

$$R_i(\mathbf{A}) \triangleq \sum_{j=1, j \neq i}^n |a_{i,j}|, \quad 1 \leq i \leq n$$

as the *deleted absolute row sums* of \mathbf{A} . Then all the eigenvalues of \mathbf{A} are in the union of n disks, i.e.

$$\lambda(\mathbf{A}) \in \bigcup_{i=1}^n G_i(\mathbf{A}),$$

where $G_i(\mathbf{A}) \triangleq \{z \in \mathbb{C}: |z - a_{ii}| \leq R_i(\mathbf{A})\}$ is the i th Gerschgorin disk. Moreover, if a union of k disks forms a connected region disjoint from all the remaining disks, then there are k eigenvalues of \mathbf{A} in this region.

By Lemma 1, the off-diagonal terms of each row in (31) are much smaller than the corresponding diagonal terms. Then, according to lemma 2, its eigenvalues are approximately $\gamma_0 + 1, \dots, \gamma_D + 1$. We will give a bound for the approximation error in the next subsection. Now we directly use this approximation to discuss the behavior of MPB. Without loss of generality, assume $\gamma_1 > \dots > \gamma_D$, then

$$\lambda_{\max} \approx \max\{\gamma_0 + 1, \gamma_1 + 1, \dots, \gamma_D + 1, 1\} = \max\{\gamma_0 + 1, \gamma_1 + 1\}. \quad (33)$$

Substituting the expression of $\mathbf{a}_0^H \mathbf{R}_T^{-1} \mathbf{a}_0$ in Lemma 1 into its definition in (32), we can have

$$\gamma_0 = (N - \beta) \frac{L \text{SNR}}{L\beta \text{SNR} + N} \quad (34)$$

which is a monotonically increasing function of SNR. Furthermore, we will show later that $\gamma_1 + 1$ is approximate to one of the generalized eigenvalue of $(\mathbf{Q}_S, \mathbf{Q}_T)$ and is almost independent of SNR. Hence, there is a threshold SNR_{T0} such that λ_{\max} switches from $\gamma_1 + 1$ to $\gamma_0 + 1$ when SNR exceeds SNR_{T0} . Its expression is in (20) and can be derived by setting (34) to γ_1 and solving SNR. As a result,

- When $\text{SNR} > \text{SNR}_{T0}$, $\lambda_{\max} \approx \gamma_0 + 1$. If $\gamma_0 + 1$ can be much greater than $\gamma_1 + 1$ as SNR increases, then (25) implies $\mathbf{w} \approx \mu_1 \mathbf{R}_T^{-1} \mathbf{a}_0$. Hence, \mathbf{a}_0 is the dominant steering vector, and the beamformer can operate properly by steering the mainlobe to the direction of the desired signal.

- When $\text{SNR} < \text{SNR}_{\text{T0}}$, $\lambda_{\max} \approx \gamma_1 + 1$. Thus $\mathbf{w} \approx \mu_1 \mathbf{R}_{\mathcal{I}}^{-1} \mathbf{a}_{\epsilon_1}$, and \mathbf{a}_{ϵ_1} is the dominant steering vector in (25). By $\mathbf{A}_{\epsilon} = \mathbf{A}_I (\mathbf{T}^{-1})^H$, \mathbf{a}_{ϵ_1} is a linear combination of all the interference steering vectors. Therefore, the beamformer fails for its mainlobe pointing to the directions of the interferers. If $\beta \neq 0$, then there would be SOI in $\mathbf{R}_{\mathcal{I}}$, which makes MPB treat it as interference and null it out. This explains the reason why $G(\text{SNR})$ decreases in the order of $\mathcal{O}(\text{SNR}^{-2})$ in Fig. 2(c).

Now, we further analyze how this threshold effect happens. By the factorizations (26), we can rewrite $\mathbf{R}_{\mathcal{S}} - \mathbf{R}_{\mathcal{I}}$ on the left hand side of (23) as

$$\mathbf{R}_{\mathcal{S}} - \mathbf{R}_{\mathcal{I}} = \gamma_0 \cdot \mathbf{a}_{S_0} \mathbf{a}_{S_0}^H + \sum_{i=1}^D \gamma_i \cdot \mathbf{a}_{\epsilon_i} \mathbf{a}_{\epsilon_i}^H, \quad (35)$$

where $\mathbf{a}_{S_0} \triangleq \mathbf{a}_0 / [\mathbf{a}_0^H \mathbf{R}_{\mathcal{I}}^{-1} \mathbf{a}_0]^{\frac{1}{2}}$. It is obvious that γ_0 is the generalized eigenvalue of the matrix pair $((\sigma_{S_0}^2 - \sigma_{\mathcal{I}_0}^2) \mathbf{a}_0 \mathbf{a}_0^H, \mathbf{R}_{\mathcal{I}})$, with $\mathbf{R}_{\mathcal{I}}^{-1} \mathbf{a}_{S_0}$ being its ‘‘normalized’’ eigenvector. By applying (29) to (28), we can also verify that $\gamma_1, \gamma_2, \dots, \gamma_D$ are the generalized eigenvalues of $(\mathbf{A}_I \Phi_{\Delta} \mathbf{A}_I^H, \mathbf{R}_{\mathcal{I}})$, with the eigenvectors being $\{\mathbf{R}_{\mathcal{I}}^{-1} \mathbf{a}_{\epsilon_i}\}_{i=1}^D$. Comparing (35) with the left hand side of (23), we can find that γ_0 actually measures the mismatch of the desired signal between the signal channel and the interference channel in Fig. 1, and $\{\gamma_i\}_{i=1}^D$ measures that of the interferers. From the previous discussion, we know that $\lambda_{\max} = \max\{\gamma_0 + 1, \gamma_1 + 1\}$, and \mathbf{w} takes $\mathbf{R}_{\mathcal{I}}^{-1} \mathbf{a}_0$ or $\mathbf{R}_{\mathcal{I}}^{-1} \mathbf{a}_{\epsilon_1}$ depending on which one of $\gamma_0 + 1$ and $\gamma_1 + 1$ is larger. Therefore, MPB *blindly* chooses the one with the largest mismatch matrix in (35) as its steering vector. We term this as ‘‘steering vector competition’’. The threshold happens when the SNR is large enough so that γ_0 exceeds γ_1 . If there is no mismatch, i.e. $\Phi_{\Delta} = \mathbf{O}$ so that $\gamma_i = 0$, then the desired signal always wins out in the competition ($\gamma_0 > \gamma_1$), and MPB can work properly for all SNR.

D. Proof of Theorem 1

Let us return to our original problem of operating curve for MPB and prove Theorem 1. We first use the expression of \mathbf{w} in (25) to derive $G(\text{SNR})$ in term of λ_{\max} . The result is given by the following lemma, with its proof in Appendix B.

Lemma 3: The normalized output SINR in (17) can be expressed as the following function of λ_{\max}

$$G(\text{SNR}) = \frac{\left[1 + \frac{N}{L\beta\text{SNR} + N} \psi_S(\lambda_{\max})\right]^2}{\left[\psi_I(\lambda_{\max}) - \frac{L\beta\text{SNR}}{L\beta\text{SNR} + N} \psi_S^2(\lambda_{\max})\right] + \left[1 + \frac{N}{L\beta\text{SNR} + N} \psi_S(\lambda_{\max})\right]^2}. \quad (36)$$

where $\psi_S(\lambda_{\max})$ and $\psi_I(\lambda_{\max})$ are in the following forms with ψ_{T_i} being the i th component of ψ_T .

$$\psi_S(\lambda_{\max}) \triangleq \frac{\sigma^2}{L} \sum_{i=1}^D \frac{\lambda_{\max} - 1}{\lambda_{\max} - (\gamma_i + 1)} |\psi_{T_i}|^2, \quad \psi_I(\lambda_{\max}) \triangleq \frac{\sigma^2}{L} \sum_{i=1}^D (\gamma_i + 1) \left[\frac{\lambda_{\max} - 1}{\lambda_{\max} - (\gamma_i + 1)} \right]^2 |\psi_{T_i}|^2. \quad (37)$$

To further simplify (36), we need the expression of λ_{\max} . In the previous subsection, we used the approximation (33) to analyze MPB. The following lemma quantifies how precise it is by bounding the approximation error. Besides checking the validity of (33), this is also critical in deriving $\mathbf{G}(\text{SNR})$.

Lemma 4: The largest generalized eigenvalue of $(\mathbf{R}_S, \mathbf{R}_T)$ defined in (4) and (5) satisfies

$$|\lambda_{\max} - (\lambda_a + 1)| \leq \lambda_a \cdot f\left(\frac{\lambda_b}{\lambda_a}\right) \quad (38)$$

where $\lambda_a \triangleq \max\{\gamma_0, \gamma_1\}$ and $\lambda_b \triangleq \min\{\gamma_0, \gamma_1\}$. $f(x)$ and δ are defined as

$$f(x) \triangleq \frac{1}{2} \left[1 - x - \sqrt{(1-x)^2 - 4\delta|x|} \right], \quad \delta \triangleq \frac{\frac{\sigma^2}{L} |\psi_{T_1}|^2}{\frac{L\beta}{N} \text{SNR} + 1} \ll 1, \quad x \in (-\infty, 1-2\gamma_-] \cup [1+2\gamma_+, +\infty)$$

with $\gamma_{\pm} \triangleq \sqrt{\delta^2 + \delta} \pm \delta$. Furthermore, $0 \leq f(x) \leq \max\{\delta, \gamma_-\} \ll 1$ when $x \in (-\infty, 1-2\gamma_-]$.

Proof: The key idea here is to design the appropriate similarity transform for \mathbf{M} in (31) and apply Lemma 2. Our detailed proof can be found in Appendix A. \square

Now we are ready to derive the expression of $\mathbf{G}(\text{SNR})$. We first consider the trivial case of $-1 \leq \gamma_1 \leq 0$.² Since $\gamma_D < \dots < \gamma_1$, we can immediately have from (37) that $0 < \psi_S(\lambda_{\max}) < \frac{\sigma^2}{L} \|\psi_T\|^2 \ll 1$ and $0 < \psi_I(\lambda_{\max}) < \frac{\sigma^2}{L} \|\psi_T\|^2 \ll 1$. Therefore, (36) becomes $\mathbf{G}(\text{SNR}) \approx 1$ for all SNR.

Next, we are going to discuss the case of $\gamma_1 > 0$ in two separate cases.

1) $\gamma_0 > \gamma_1$: Then $\lambda_a = \gamma_0$, $\lambda_b = \gamma_1$ and $\lambda_{\max} \approx \gamma_0 + 1$. So long as SNR is slightly larger than SNR_{T_0} such that $\gamma_0 > \gamma_1 / (1 - \sqrt{\sigma^2/L} \|\psi_T\|) \approx \gamma_1$, we have the following approximation for ψ_S :

$$\psi_S(\lambda_{\max}) \approx \frac{\sigma^2}{L} \sum_{i=1}^D \frac{\gamma_0}{\gamma_0 - \gamma_i} |\psi_{T_i}|^2 < \frac{\gamma_0}{\gamma_0 - \gamma_1} \frac{\sigma^2}{L} \sum_{i=1}^D |\psi_{T_i}|^2 < \sqrt{\frac{\sigma^2}{L}} \|\psi_T\| \ll 1.$$

Moreover, we approximate ψ_I by the following bound, which is asymptotically tight with respect to $\frac{\gamma_0}{\gamma_1}$.³

$$\psi_I(\lambda_{\max}) \approx \frac{\sigma^2}{L} \sum_{i=1}^D (\gamma_i + 1) \left(\frac{\gamma_0}{\gamma_0 - \gamma_i} \right)^2 |\psi_{T_i}|^2 \leq \left(\frac{\gamma_0}{\gamma_0 - \gamma_1} \right)^2 \frac{\sigma^2}{L} \sum_{i=1}^D (\gamma_i + 1) |\psi_{T_i}|^2.$$

Substituting the above two approximations together with (34) and (20) into (36), we can finally have

$$\mathbf{G}(\text{SNR}) = \frac{P_I + 1}{P_I / [1 - \text{SNR}_{T_0} / \text{SNR}]^2 + 1} G_U$$

where $G_U = 1 / (P_I + 1)$ and P_I is defined as

$$P_I \triangleq \left[\frac{(N - \beta) / \beta}{(N - \beta) / \beta - \gamma_1} \right]^2 \frac{\sigma^2}{L} \sum_{i=1}^D (\gamma_i + 1) |\psi_{T_i}|^2$$

²Since γ_i is the eigenvalue of $(\mathbf{A}_I \Phi_{\Delta} \mathbf{A}_I^H, \mathbf{R}_T)$, $\gamma_i + 1$ is for $(\sigma_{x_0}^2 \mathbf{a}_0 \mathbf{a}_0^H + \mathbf{Q}_S, \mathbf{R}_T)$, a positive definite pair. Hence $\gamma_i + 1 > 0$.

³In fact, this approximation is precise enough when γ_0 is reasonably larger than γ_1 , say, $\gamma_0 > 2\gamma_1$.

However, this expression is difficult to evaluate. Instead, we can compute G_U first and have $P_I=1/G_U-1$. Noticing that G_U is the output SINR as $\text{SNR}=\infty$, we can ignore the term $\mathbf{A}_I\Phi_{\Delta}\mathbf{A}_I^H$ on the left hand side of (23). Hence, $\mathbf{w}_{\infty}=\mu\mathbf{R}_{\mathcal{I}}^{-1}\mathbf{a}_0=\mu'\mathbf{Q}_{\mathcal{I}}^{-1}\mathbf{a}_0$, and by (17) and (14), we have its expression in (19).

2) $\gamma_0 < \gamma_1$: Then $\lambda_a=\gamma_1$, $\lambda_b=\gamma_0$ and $\lambda_{\max}\approx\gamma_1+1$. As a result, the term corresponding to γ_1 would dominate ψ_S and ψ_I in (37). To further evaluate these two terms, we need the bound in (38) to measure how close λ_{\max} is to γ_1+1 , namely, we use it to evaluate $\lambda_{\max}-(\gamma_1+1)$ in ψ_S and ψ_I :

$$\begin{aligned}\psi_S(\lambda_{\max}) &\approx \frac{\sigma^2}{L} \frac{\gamma_1}{\lambda_{\max}-(\gamma_1+1)} |\psi_{T_1}|^2 \approx \frac{\sigma^2}{L} \frac{1}{f\left(\frac{\gamma_0}{\gamma_1}\right)} |\psi_{T_1}|^2 = \left(\frac{L\beta}{N}\text{SNR}+1\right) \frac{\gamma_1}{\gamma_0} \cdot g\left(\frac{\gamma_0}{\gamma_1}\right) \\ \psi_I(\lambda_{\max}) &\approx \frac{\sigma^2}{L} \frac{(\gamma_1+1)\gamma_1^2}{[\lambda_{\max}-(\gamma_1+1)]^2} |\psi_{T_1}|^2 \approx \frac{\sigma^2}{L} \frac{\gamma_1+1}{\left[f\left(\frac{\gamma_0}{\gamma_1}\right)\right]^2} |\psi_{T_1}|^2 = \frac{\gamma_1+1}{\frac{\sigma^2}{L}|\psi_{T_1}|^2} [\psi_S(\lambda_{\max})]^2\end{aligned}$$

where $g(x) = \frac{1}{2}[1-x+\sqrt{(1-x)^2-4\delta x}]$. In fact, we can have the approximation that $g(x) \approx 1-x$, because

$$|(1-x) - g(x)| = |f(x)| \ll 1$$

Substituting the above expressions of ψ_S and ψ_I as well as the approximation of $g(x)$ into (3), we get

$$\mathbf{G}(\text{SNR}) = \left[\frac{N}{L\beta\text{SNR}+N} \right]^2 \left[\frac{\gamma_1}{\gamma_1-\gamma_0} \right]^2 \left[\frac{\gamma_1+1}{\frac{\sigma^2}{L}|\psi_{T_1}|^2} - \frac{L\beta}{N}\text{SNR} + \left(\frac{\gamma_1}{\gamma_1-\gamma_0} \right)^2 \right]^{-1} \approx \left[\frac{N}{L\beta\text{SNR}+N} \right]^2 \left[\frac{\gamma_1}{\gamma_1-\gamma_0} \right]^2 G_L,$$

where $G_L \triangleq \frac{\sigma^2}{L}|\psi_{T_1}|^2/(\gamma_1+1)$ is the output SINR when $\text{SNR}=0$ ($-\infty$ dB). The last approximation holds when $\gamma_0 < (1-\sqrt{\frac{\sigma^2}{L}|\psi_{T_1}|^2})\gamma_1$, i.e. γ_0 is slightly smaller than γ_1 , which implies $\gamma_1^2/(\gamma_1-\gamma_0)^2 < 1/\frac{\sigma^2}{L}|\psi_{T_1}|^2 < (\gamma_1+1)/\frac{\sigma^2}{L}|\psi_{T_1}|^2$. Furthermore, because $\frac{\sigma^2}{L}|\psi_{T_1}|^2 \ll 1$, $\frac{L\beta}{N}\text{SNR}/(\frac{L\beta}{N}\text{SNR}+1) < 1 \ll (\gamma_1+1)/\frac{\sigma^2}{L}|\psi_{T_1}|^2$. There is, however, no easier way to evaluate G_L than its definition. Fortunately, we are not interested in its specific values but the threshold SNR_{T_1} that \mathbf{G} reaches this value, as discussed in Sec. III-A. Noticing that $\text{SNR}_{T_0} = \infty$ when $(N-\beta)/\beta < \gamma_1$ (c.f. (20)), we have following fact regarding γ_1 and SNR_{T_0} ,

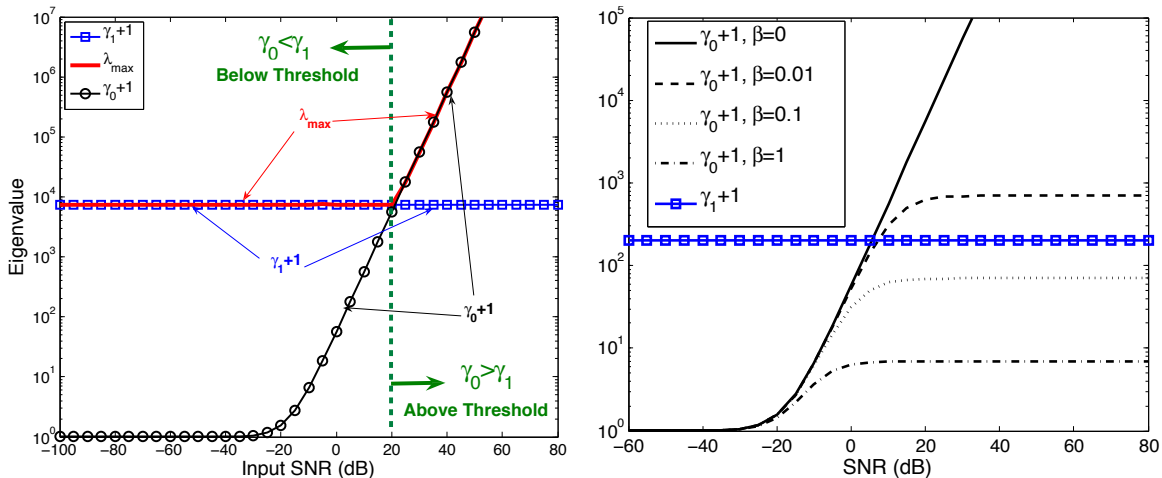
$$\gamma_1 = \frac{L(N-\beta)\text{SNR}_{T_0}}{L\beta\text{SNR}_{T_0}+N} + \left(\gamma_1 - \frac{N-\beta}{\beta} \right)^+.$$

Combining the above expression and (34), $\mathbf{G}(\text{SNR})$ can be reduced to

$$\mathbf{G}(\text{SNR}) = \left[\frac{1+K_0}{1-\text{SNR}/\text{SNR}_{T_0}+K_0\left(\frac{L\beta}{N}\text{SNR}+1\right)} \right]^2 G_L \quad (39)$$

with K_0 defined in (21). Finally, the following lemma provides an easier way to compute SNR_{T_0} from γ_1 . The proof can also be found in Appendix A.

Lemma 5: $\gamma_1, \dots, \gamma_D$ are approximate to all the nonzero generalized eigenvalues of $(\mathbf{Q}_S-\mathbf{Q}_I, \mathbf{Q}_I)$ (padded up to D with zeros if not enough), and is almost independent of SNR .

(a) The curves of γ_0+1 , γ_1+1 and λ_{\max} vs. SNR. ($\beta = 0$)(b) γ_0+1 against SNR with different β .Fig. 3. The curve of $\gamma_0 + 1$ and $\gamma_1 + 1$ against SNR. The intersection of them is the empirical threshold SNR_{T_0} .

IV. DISCUSSION OF THE THRESHOLD

From Theorem 1 in Sec. III-A, we know that the empirical threshold SNR_{T_0} is a key parameter for MPB. By the discussion in Sec. III-C, it is the intersection of the curves γ_0+1 and γ_1+1 , as shown in Fig. 3(a). Therefore, we need to investigate these two parameters to gain deeper insight of SNR_{T_0} .

A. General Results of γ_0 and γ_1

γ_0 has a simple expression of (34), from which we know that the parameter β is critical. Fig. 3(b) shows the curve of γ_0+1 with different β . We see that, if $\beta = 0$, i.e. \mathbf{H}_I and \mathbf{h}_S are orthogonal, then $\gamma_0 = L \text{SNR}$ is unbounded as SNR goes to infinity. Otherwise, there would be a limiting value of $(N-\beta)/\beta$ so that γ_0 might never exceed γ_1 and $\text{SNR}_{T_0} = +\infty$. Therefore, $\beta=0$ is the best choice for γ_0 .

γ_1 is another critical parameter that determines SNR_{T_0} . Fig. 3 shows that, as γ_1 increases, its intersection with γ_0 moves rightward and SNR_{T_0} increases. Therefore, knowing how to control γ_1 is important in designing MPB. By Lemma 5, γ_1 is the largest nonzero generalized eigenvalue of $(\mathbf{Q}_S - \mathbf{Q}_I, \mathbf{Q}_I)$. (It is zero if there are less than D nonzero eigenvalues and all of them are negative.) To solve it directly, we need the roots of a polynomial eigen-equation of order L , which has no general formula when $L > 4$. Instead, we resort to matrix perturbation theory again to derive a bound for it. We first notice that the eigen-decomposition of $(\mathbf{Q}_S - \mathbf{Q}_I, \mathbf{Q}_I)$ is equivalent to $(\mathbf{Q}_S, \mathbf{Q}_I)$ and their eigenvalues only differ by

one. By (6) and (7), the eigenvalue of $(\mathbf{Q}_S, \mathbf{Q}_I)$ is further equivalent to that of $(\mathbf{Y}_S + \mathbf{I}, \mathbf{Y}_I + \mathbf{I})$, where

$$\mathbf{Y}_S = \frac{1}{\sigma^2} \mathbf{A}_I \Phi_S \mathbf{A}_I^H = \text{INR} \cdot \mathbf{A}_I \Phi_{S_0} \mathbf{A}_I^H, \quad \mathbf{Y}_I = \frac{1}{\sigma^2} \mathbf{A}_I \Phi_I \mathbf{A}_I^H = \text{INR} \cdot \mathbf{A}_I \Phi_{I_0} \mathbf{A}_I^H. \quad (40)$$

We term $(\mathbf{Y}_S, \mathbf{Y}_I)$ as *noise free pair*, since it can be viewed as the covariance matrix pair of MPB without noise. Our strategy here is to view $(\mathbf{Y}_S + \mathbf{I}, \mathbf{Y}_I + \mathbf{I})$ as a perturbed version of $(\mathbf{Y}_S, \mathbf{Y}_I)$ and apply the results in matrix perturbation theory to derive a bound for $\gamma_1 + 1$. Before we proceed on, we cite a more general definition of the generalized eigenvalue of a matrix pair [32].

Definition 2 (Generalized eigenvalue): The generalized eigenvalue of a matrix pair (\mathbf{A}, \mathbf{B}) is a one dimensional space, denoted as $\langle \nu, \mu \rangle \triangleq \{ \tau \cdot [\nu \ \mu] : \tau \in \mathbb{C} \}$, where $[\nu \ \mu]$ is a 1×2 vector satisfying

$$\mu \cdot \mathbf{A} \mathbf{x} = \nu \cdot \mathbf{B} \mathbf{x},$$

with \mathbf{x} being its eigenvector. If \mathbf{B} is nonsingular, then $\lambda = \nu / \mu$ becomes the conventional definition.

Comparing to the conventional definition of generalized eigenvalues, this one includes the special case of \mathbf{B} being singular so that $\mu = 0$ and $\nu \neq 0$, namely, $\lambda = +\infty$. We will see its importance later. Besides, we also need the following definition and lemma from [32, pp.315–316].

Definition 3 (Definite pair): If a matrix pair (\mathbf{A}, \mathbf{B}) consists of two Hermitian matrices and

$$C(\mathbf{A}, \mathbf{B}) \triangleq \min_{\|\mathbf{x}\|=1} \sqrt{(\mathbf{x}^H \mathbf{A} \mathbf{x})^2 + (\mathbf{x}^H \mathbf{B} \mathbf{x})^2} > 0,$$

then (\mathbf{A}, \mathbf{B}) is called definite pair, and $C(\mathbf{A}, \mathbf{B})$ is its Crawford number.

Theorem 2 (Weyl-Lidskii type): Assume (\mathbf{A}, \mathbf{B}) is a definite pair and $(\mathbf{A} + \mathbf{E}, \mathbf{B} + \mathbf{F})$ is its perturbed version. Let $\langle \alpha_i, \beta_i \rangle$ and $\langle \tilde{\alpha}_i, \tilde{\beta}_i \rangle$, ($i=1, \dots, n$), be their ordered generalized eigenvalues, respectively. If

$$\sqrt{\|\mathbf{E}\|_S^2 + \|\mathbf{F}\|_S^2} < C(\mathbf{A}, \mathbf{B}), \quad (41)$$

where $\|\cdot\|_S$ denotes spectral norm of a matrix, then $(\tilde{\mathbf{A}}, \tilde{\mathbf{B}})$ is a definite pair, and

$$\frac{|\alpha_1 \tilde{\beta}_2 - \beta_1 \tilde{\alpha}_2|}{\sqrt{|\alpha_1|^2 + |\beta_1|^2} \sqrt{|\tilde{\alpha}_2|^2 + |\tilde{\beta}_2|^2}} \leq \frac{\sqrt{\|\mathbf{E}\|_S^2 + \|\mathbf{F}\|_S^2}}{C(\mathbf{A}, \mathbf{B})},$$

We want to apply Theorem 2 to $(\mathbf{Y}_S + \mathbf{I}, \mathbf{Y}_I + \mathbf{I})$ and $(\mathbf{Y}_S, \mathbf{Y}_I)$ to derive a bound for its eigenvalues. However, $(\mathbf{Y}_S, \mathbf{Y}_I)$ is not a definite pair, for the null spaces of \mathbf{Y}_S and \mathbf{Y}_I may have nontrivial interset (larger than $\{0\}$). Therefore, we need to transform $(\mathbf{Y}_S, \mathbf{Y}_I)$ into a definite pair. Let \mathcal{N}_S and \mathcal{N}_I be the null spaces of \mathbf{Y}_S and \mathbf{Y}_I , respectively, and $\mathcal{N}_0 \triangleq \mathcal{N}_S \cap \mathcal{N}_I$. Let \mathbf{E}_0 be a matrix whose columns are the orthonormal basis of \mathcal{N}_0^\perp , with $\mathbf{E}_0^H \mathbf{E}_0 = \mathbf{I}$. Then, by the determinant identity in (29), $(\mathbf{Y}_S + \mathbf{I}, \mathbf{Y}_I + \mathbf{I})$ has the same generalized eigenvalues as $(\mathbf{E}_0^H \mathbf{Y}_S \mathbf{E}_0 + \mathbf{I}, \mathbf{E}_0^H \mathbf{Y}_I \mathbf{E}_0 + \mathbf{I})$, except for the

multiplicity of ones. Similarly, $(\mathbf{E}_0^H \mathbf{Y}_S \mathbf{E}_0, \mathbf{E}_0^H \mathbf{Y}_I \mathbf{E}_0)$ has the same eigenvalue as $(\mathbf{Y}_S, \mathbf{Y}_I)$ does except for the multiplicity of zero. Therefore, instead, we can apply Theorem 2 to $(\mathbf{E}_0^H \mathbf{Y}_S \mathbf{E}_0, \mathbf{E}_0^H \mathbf{Y}_I \mathbf{E}_0)$ and $(\mathbf{E}_0^H \mathbf{Y}_S \mathbf{E}_0 + \mathbf{I}, \mathbf{E}_0^H \mathbf{Y}_I \mathbf{E}_0 + \mathbf{I})$ to derive the bound. The Crawford number of $(\mathbf{E}_0^H \mathbf{Y}_S \mathbf{E}_0, \mathbf{E}_0^H \mathbf{Y}_I \mathbf{E}_0)$ is

$$C_Y = \min_{\mathbf{w} \in \mathcal{N}_0^\perp, \|\mathbf{w}\|=1} \sqrt{(\mathbf{w}^H \mathbf{Y}_S \mathbf{w})^2 + (\mathbf{w}^H \mathbf{Y}_I \mathbf{w})^2} > 0, \quad (42)$$

which means $(\mathbf{E}_0^H \mathbf{Y}_S \mathbf{E}_0, \mathbf{E}_0^H \mathbf{Y}_I \mathbf{E}_0)$ is a positive pair. Before applying Theorem 2, we first analyze the dependency of C_Y on the interference power. Substituting (40) into (42), we have $C_Y = \text{INR} \cdot C_{Y_0}$, where

$$C_{Y_0} = \min_{\mathbf{w} \in \mathcal{N}_0^\perp, \|\mathbf{w}\|=1} \sqrt{(\mathbf{w}^H \mathbf{A}_I \Phi_{S_0} \mathbf{A}_I^H \mathbf{w})^2 + (\mathbf{w}^H \mathbf{A}_I \Phi_{I_0} \mathbf{A}_I^H \mathbf{w})^2}.$$

Since Φ_{S_0} and Φ_{I_0} are independent of INR (c.f. Sec. II-B), C_{Y_0} is also independent of INR. Therefore, C_Y is proportional to INR. Now, we are ready to use Theorem 2, and we only consider the case of INR being large. Let $\langle \nu_0, \mu_0 \rangle$ and $\langle \nu, \mu \rangle$ be the corresponding generalized eigenvalues of $(\mathbf{E}_0^H \mathbf{Y}_S \mathbf{E}_0, \mathbf{E}_0^H \mathbf{Y}_I \mathbf{E}_0)$ and $(\mathbf{E}_0^H \mathbf{Y}_S \mathbf{E}_0 + \mathbf{I}, \mathbf{E}_0^H \mathbf{Y}_I \mathbf{E}_0 + \mathbf{I})$, respectively. Then, for large INR, (41) is satisfied and

$$\frac{|\nu\mu_0 - \mu\nu_0|}{\sqrt{|\nu|^2 + |\mu|^2} \sqrt{|\nu_0|^2 + |\mu_0|^2}} < \frac{\sqrt{2}}{C_{Y_0}} \cdot \frac{1}{\text{INR}}. \quad (43)$$

We now derive the bound for $\gamma_1 + 1$ in two separate cases.

1) $\mathcal{N}_I \not\subseteq \mathcal{N}_S$: There is a nonzero \mathbf{w}_0 such that $\mathbf{Y}_S \mathbf{w}_0 \neq \mathbf{0}$ and $\mathbf{Y}_I \mathbf{w}_0 = \mathbf{0}$. By Definition 2, $\langle \nu_0, 0 \rangle$ ($\forall \nu_0 \neq 0$) is a generalized eigenvalue of $(\mathbf{Y}_S, \mathbf{Y}_I)$ and $(\mathbf{E}_0^H \mathbf{Y}_S \mathbf{E}_0, \mathbf{E}_0^H \mathbf{Y}_I \mathbf{E}_0)$. This means the noise free pair $(\mathbf{Y}_S, \mathbf{Y}_I)$ has an infinite generalized eigenvalue. As a result, (43) becomes

$$\frac{|\mu|}{\sqrt{|\nu|^2 + |\mu|^2}} < \frac{\sqrt{2}}{C_{Y_0}} \cdot \frac{1}{\text{INR}} \quad \Leftrightarrow \quad \lambda \triangleq \frac{\nu}{\mu} > \sqrt{\frac{C_{Y_0}^2}{2} \text{INR}^2 - 1} \approx \frac{C_{Y_0}}{\sqrt{2}} \text{INR}.$$

This means $(\mathbf{E}_0^H \mathbf{Y}_S \mathbf{E}_0 + \mathbf{I}, \mathbf{E}_0^H \mathbf{Y}_I \mathbf{E}_0 + \mathbf{I})$ would always have an eigenvalue that satisfies the above inequality. Since $(\mathbf{Q}_S, \mathbf{Q}_I)$ has the same eigenvalue except for the multiplicity of ones, $\gamma_1 + 1$ satisfies

$$\gamma_1 + 1 > \frac{C_{Y_0}}{\sqrt{2}} \text{INR}, \quad (44)$$

which gives a lower bound for $\gamma_1 + 1$. We can see that it goes up unboundedly as INR increases. Hence, by (20) and (22), the threshold SNR also increases unboundedly with INR.

2) $\mathcal{N}_I \subseteq \mathcal{N}_S$: Then, $\mathcal{N}_0 = \mathcal{N}_I$ and $\mathbf{E}_0^H \mathbf{Y}_I \mathbf{E}_0$ is nonsingular. As a result, all eigenvalues of $(\mathbf{E}_0^H \mathbf{Y}_S \mathbf{E}_0, \mathbf{E}_0^H \mathbf{Y}_I \mathbf{E}_0)$ and $(\mathbf{Y}_S, \mathbf{Y}_I)$ are bounded. When INR is large, (43) becomes

$$\frac{|\lambda - \lambda_0|}{\sqrt{1 + \lambda^2} \sqrt{1 + \lambda_0^2}} < \frac{C_{Y_0}}{\sqrt{2}} \cdot \frac{1}{\text{INR}} \quad \Rightarrow \quad |\lambda - \lambda_0| < \frac{C_{Y_0}}{\sqrt{2}} (1 + \lambda_0^2) \cdot \frac{1}{\text{INR}}$$

where $\lambda_0 = \nu_0 / \mu_0$ is the largest eigenvalue of $(\mathbf{E}_0^H \mathbf{Y}_S \mathbf{E}_0, \mathbf{E}_0^H \mathbf{Y}_I \mathbf{E}_0)$ and we used $\lambda \approx \lambda_0$ in the second inequality. Since $(\mathbf{Q}_S, \mathbf{Q}_I)$ has the same eigenvalue as $(\mathbf{E}_0^H \mathbf{Y}_S \mathbf{E}_0 + \mathbf{I}, \mathbf{E}_0^H \mathbf{Y}_I \mathbf{E}_0 + \mathbf{I})$ except for the

multiplicity of ones, $\gamma_1 + 1$ is bounded around the largest eigenvalue of $(\mathbf{Y}_S, \mathbf{Y}_I)$ or one. Furthermore, from (40), we know that λ_0 is independent of INR. Therefore, as all eigenvalues of noise free pair is finite, $\gamma_1 + 1$ is bounded and independent of INR.

B. Two Typical Scenarios of γ_1

From the previous part, we know that whether the threshold of MPB is unbounded is determined by the existence of infinite eigenvalue of the noise free pair. Now, we discuss two typical classes of interferences. In the first case, all eigenvalues are finite, and in the second case, there may be infinite eigenvalues.

1) *Directional White Noise*: By uncorrelated directional white noise, we mean an interference that arrives from a specific direction, with its samples in time domain being uncorrelated. This means the entries of $\mathbf{S}_I(k)$ are independent identically distributed random variables with zero mean and unit variance. (In section II-A, we have already normalized the interference power in $s_i(k)$.) Then, by (8), we can immediately have $\Phi_{S_0} = \Phi_{I_0}$, and all the eigenvalue of the noise free pair $(\mathbf{Y}_S, \mathbf{Y}_I)$ are ones. Thus, in this case, $\gamma_1 + 1$ is bounded and is independent of INR. In fact, we can further have $\mathbf{Q}_S = \mathbf{Q}_I$ according to (6) and (7). Therefore, $\gamma_1 = 0$, $\text{SNR}_{T_0} = 0$ and $\mathbf{G}(\text{SNR}) = 1$.

2) *Directional Periodical Interference*: If an interference has periodical structure in time domain and arrives from certain direction, then we term it as directional periodical interference. By periodical, we mean the interfer is periodic with respect to the projection basis, i.e.

$$\mathbf{H}_I^H \mathbf{S}_I(k) = e^{j\phi_k} \mathbf{H}_I^H \mathbf{S}_I, \quad \mathbf{h}_S^H \mathbf{S}_I(k) = e^{j\phi'_k} \mathbf{h}_S^H \mathbf{S}_I. \quad (45)$$

A stronger condition would be $\mathbf{S}_I(k) = \mathbf{S}_I$. However, (45) is good enough for our analysis. Now, we will discuss the existence of infinite generalized eigenvalue in the noise free pair $(\mathbf{Y}_S, \mathbf{Y}_I)$. To do this, we need to consider the relationship between their null spaces.

In practice, \mathbf{R}_S and \mathbf{R}_I are estimated from sample average. Therefore, replacing the expectation in (8) by sample average and using (45), we can get

$$\Phi_{S_0} = \Omega_I^{1/2} \mathbf{S}_I^T \mathbf{h}_S^* \mathbf{h}_S^T \mathbf{S}_I^* \Omega_I^{1/2}, \quad \Phi_{I_0} = \frac{1}{r_I} \Omega_I^{1/2} \mathbf{S}_I^T \mathbf{H}_I^* \mathbf{H}_I^T \mathbf{S}_I^* \Omega_I^{1/2}.$$

Let $\mathbf{\Pi} \triangleq \mathbf{S}_I \Omega_I^{1/2} \mathbf{A}_I^T$. Then, by (40), \mathbf{Y}_S and \mathbf{Y}_I in this case can be expressed as

$$\mathbf{Y}_S = \text{INR} \cdot (\mathbf{\Pi}^H \mathbf{h}_S \mathbf{h}_S^H \mathbf{\Pi})^*, \quad \mathbf{Y}_I = \text{INR} \cdot \frac{1}{r_I} (\mathbf{\Pi}^H \mathbf{H}_I \mathbf{H}_I^H \mathbf{\Pi})^*. \quad (46)$$

Therefore, the noise free pair $(\mathbf{Y}_S, \mathbf{Y}_I)$ has the same eigenvalue as $(\mathbf{\Pi}^H \mathbf{h}_S \mathbf{h}_S^H \mathbf{\Pi}, \frac{1}{r_I} \mathbf{\Pi}^H \mathbf{H}_I \mathbf{H}_I^H \mathbf{\Pi})$ does, and we only have to check the null spaces of later matrix pair. Let $\mathcal{V}_I \triangleq \mathcal{R}(\mathbf{\Pi})$ be the range space of $\mathbf{\Pi}$.

By definition, it is also the range space of \mathbf{S}_I , namely the space spanned by all interference waveforms in one period. Then, we can express the null spaces of $\mathbf{\Pi}^H \mathbf{h}_S \mathbf{h}_S^H \mathbf{\Pi}$ and $\mathbf{\Pi}^H \mathbf{H}_I \mathbf{H}_I^H \mathbf{\Pi}$ as

$$\begin{aligned}\mathcal{N}'_S &\triangleq \mathcal{N}(\mathbf{\Pi}^H \mathbf{h}_S \mathbf{h}_S^H \mathbf{\Pi}) = \left\{ \mathbf{\Pi}^\dagger \mathbf{x} : \mathbf{x} \in \mathcal{S}^\perp \cap \mathcal{V}_I \right\} \oplus \mathcal{N}(\mathbf{\Pi}) \\ \mathcal{N}'_I &\triangleq \mathcal{N}(\mathbf{\Pi}^H \mathbf{H}_I \mathbf{H}_I^H \mathbf{\Pi}) = \left\{ \mathbf{\Pi}^\dagger \mathbf{x} : \mathbf{x} \in \mathcal{I}^\perp \cap \mathcal{V}_I \right\} \oplus \mathcal{N}(\mathbf{\Pi}),\end{aligned}$$

where $\mathcal{S} = \mathcal{R}(\mathbf{h}_S)$, $\mathcal{I} = \mathcal{R}(\mathbf{H}_I)$ as defined in Sec. II-B, and \dagger denotes Moore-Penrose pseudoinverse [34]. To see the relationship between \mathcal{N}'_S and \mathcal{N}'_I , we only need to check the relationship between $\mathcal{S}^\perp \cap \mathcal{V}_I$ and $\mathcal{I}^\perp \cap \mathcal{V}_I$ which can be expressed as

$$\mathcal{S}^\perp \cap \mathcal{V}_I = \{ \mathbf{x} : \mathbf{B}_S^H \mathbf{x} = \mathbf{0} \}, \quad \mathcal{I}^\perp \cap \mathcal{V}_I = \{ \mathbf{x} : \mathbf{B}_I^H \mathbf{x} = \mathbf{0} \}, \quad (47)$$

where

$$\mathbf{B}_I \triangleq \begin{bmatrix} \mathbf{H}_{\mathcal{V}_I^\perp} & \mathbf{H}_I \end{bmatrix}, \quad \mathbf{B}_S \triangleq \begin{bmatrix} \mathbf{H}_{\mathcal{V}_I^\perp} & \mathbf{h}_S \end{bmatrix}.$$

with $\mathbf{H}_{\mathcal{V}_I^\perp}$ being the matrix whose columns are the orthonormal basis of \mathcal{V}_I^\perp . Then, by (47), whether the eigenvalues of $(\mathbf{Y}_S, \mathbf{Y}_I)$ are finite is equivalent to the validity of $\mathcal{R}\{\mathbf{B}_I\} \supseteq \mathcal{R}\{\mathbf{B}_S\}$. Define

$$\mathbf{T}_{\mathbf{B}_I} \triangleq \begin{bmatrix} \mathbf{I} & -\mathbf{H}_{\mathcal{V}_I^\perp}^H \mathbf{H}_I \\ 0 & \mathbf{I} \end{bmatrix}, \quad \mathbf{T}_{\mathbf{B}_S} \triangleq \begin{bmatrix} \mathbf{I} & -\mathbf{H}_{\mathcal{V}_I^\perp}^H \mathbf{h}_S \\ 0 & \mathbf{I} \end{bmatrix}.$$

Right-multiplying \mathbf{B}_I and \mathbf{B}_S by $\mathbf{T}_{\mathbf{B}_I}$ and $\mathbf{T}_{\mathbf{B}_S}$, respectively, we can have

$$\mathbf{B}_I \cdot \mathbf{T}_{\mathbf{B}_I} = \begin{bmatrix} \mathbf{H}_{\mathcal{V}_I^\perp} & \mathbf{P}_{\mathcal{V}_I} \mathbf{H}_I \end{bmatrix}, \quad \mathbf{B}_S \cdot \mathbf{T}_{\mathbf{B}_S} = \begin{bmatrix} \mathbf{H}_{\mathcal{V}_I^\perp} & \mathbf{P}_{\mathcal{V}_I} \mathbf{h}_S \end{bmatrix},$$

where $\mathbf{P}_{\mathcal{V}_I} \triangleq \mathbf{H}_{\mathcal{V}_I} \mathbf{H}_{\mathcal{V}_I}^H$ is the projection matrix onto \mathcal{V}_I . Since $\mathbf{T}_{\mathbf{B}_I}$ and $\mathbf{T}_{\mathbf{B}_S}$ are nonsingular, the above two matrices have the same range spaces as \mathbf{B}_S and \mathbf{B}_I do, namely we can have

$$\mathcal{R}\{\mathbf{B}_I\} = \mathcal{V}_I^\perp \oplus \mathcal{R}\{\mathbf{P}_{\mathcal{V}_I} \mathbf{H}_I\}, \quad \mathcal{R}\{\mathbf{B}_S\} = \mathcal{V}_I^\perp \oplus \mathcal{R}\{\mathbf{P}_{\mathcal{V}_I} \mathbf{h}_S\}$$

Therefore, whether the generalized eigenvalues of the noise free pair are bounded is finally equivalent to whether

$$\mathcal{R}\{\mathbf{P}_{\mathcal{V}_I} \mathbf{H}_I\} \supseteq \mathcal{R}\{\mathbf{P}_{\mathcal{V}_I} \mathbf{h}_S\}. \quad (48)$$

Fig. 4 shows the geometrical interpretation of (48). To see if γ_1 is bounded, we can project \mathbf{h}_S and all the columns of \mathbf{H}_I onto \mathcal{V}_I . If the former projection lies in the space spanned by the later ones, then γ_1 is bounded. Otherwise, there is an infinite eigenvalue in the noise free pair and γ_1 will increase unboundedly with INR. Since \mathbf{H}_I of the Maximin scheme and PAPC scheme has only one column, this means the projections of \mathbf{h}_S and \mathbf{H}_I should be on the same line, which is hardly valid. Thus, these two

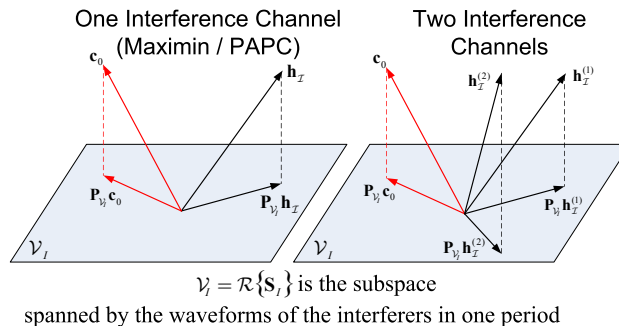


Fig. 4. Geometrical interpretation of (48). $\mathbf{h}_{\mathcal{I}}^{(1)}$ and $\mathbf{h}_{\mathcal{I}}^{(2)}$ denote the columns of $\mathbf{H}_{\mathcal{I}}$. For one interference channel, $\mathbf{H}_{\mathcal{I}} = \mathbf{h}_{\mathcal{I}}$.

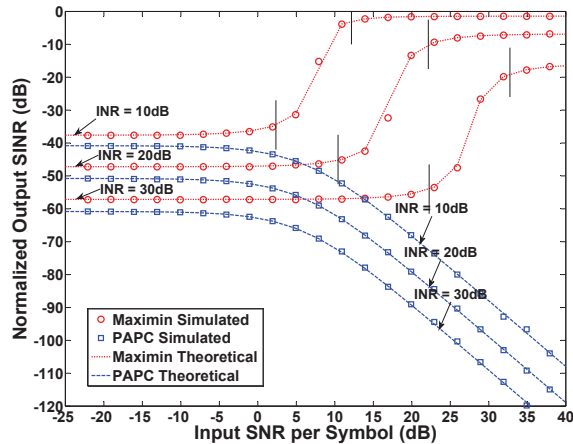
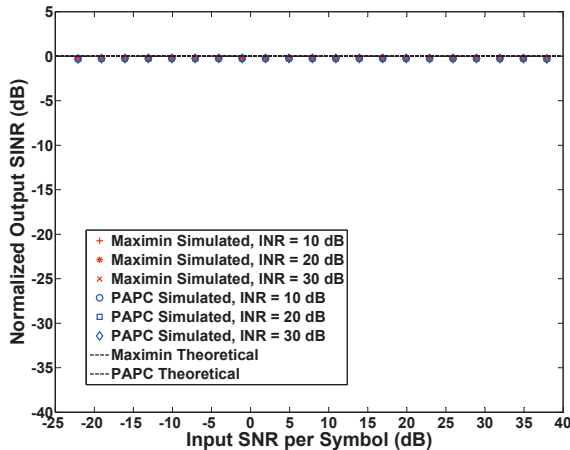
approaches are sensitive to directional periodical interferences, as we will see in later simulation results. Furthermore, Fig. 4 also shows the case of multiple interference channels, i.e. the dimension of \mathcal{I} is larger than one, then γ_1 is more likely to be bounded. This issue is out of the scope of this paper and will be discussed in in [36].

V. SIMULATION RESULTS

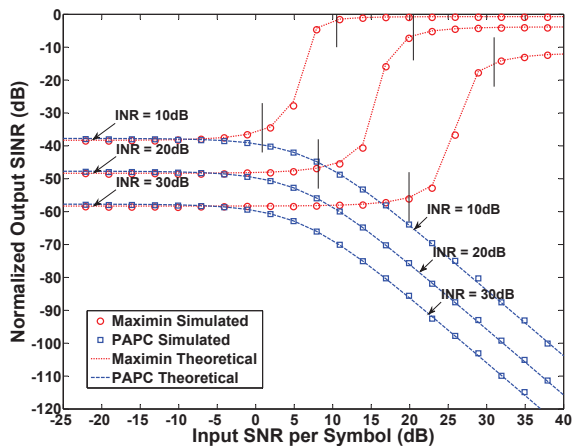
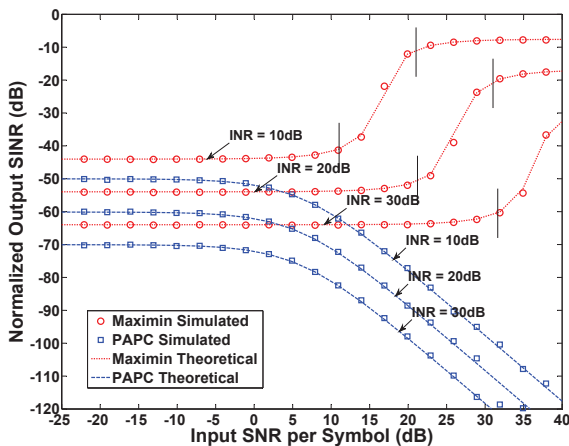
In this section, we simulate various scenarios and compare them to our theoretical results. The matrix pair beamformers implemented include the Maximin algorithm and PAPC algorithm, which have many kinds of adaptive algorithms. However, we are only interested in their steady state performance. The reason for this is that, if the methods suffer from poor steady state performance, then it is meaningless to investigate their adaptive algorithms. Therefore, we directly calculate their weight vectors by performing generalized eigen-decompositions on the estimated matrix pairs. The interference signals encountered in the simulation include BPSK signal, tones, periodical noise and multiuser interference. The first one is the directional white noise and the others are directional periodical interferences.

In all cases, we consider a uniform linear array (ULA) with eight isotropic antennas ($L = 8$) spaced half a wavelength apart. For each user, a 100 kbps DPSK signal is randomly generated and spreaded by a distinct 31-chip Gold sequence in each simulation trial. Then it is modulated onto a 1 GHz carrier to form a RF signal with bandwidth 3.1 MHz. In all the simulations, we assume the SOI arrives from 0° and the interferers have equal power.

Fig. 5(a)–Fig. 5(d) show the operating curve $G(\text{SNR})$ of the Maximin and PAPC beamformers in the four scenarios. The simulated values are obtained by using the simulated data and the theoretical ones are computed by the piecewise function $G(\text{SNR})$ in (18). To eliminate the randomness caused by finite sample effects, $K = 10^6$ symbols are simulated for each SNR and INR in every experiment.



(a) $G(\text{SNR})$ of Maximin and PAPC under BPSK jammers. (b) $G(\text{SNR})$ of Maximin and PAPC under periodical noise.



(c) $G(\text{SNR})$ of Maximin and PAPC under tone jammers. (d) $G(\text{SNR})$ of Maximin and PAPC under multipath MAI.

Fig. 5. Simulated and theoretical operating curve $G(\text{SNR})$ under different kinds of interference for Maximin and PAPC.

In Fig. 5(a), the interferers are three uncorrelated BPSK modulated signals, i.e. random sequences of ± 1 . The rates of the interferers are all 3.1Mbps, which is the same as the chip rate of the SOI and covers its whole bandwidth. Therefore, they belong to the type of directional white noise. We can see that $G(\text{SNR}) \approx 1$ and there is no threshold effect, which is consistent with the analysis in Section IV-B1.

Fig. 5(b)–Fig. 5(d) show the results for three types of directional periodical interferences: periodical noise, tones and multiple access interference (MAI) with multipath. In Fig. 5(b), we consider two periodical noises, which arrives from 30° and -40° , respectively, and each of them is generated by repeating a segment of Gaussian white noise over times, with the repeating frequency being 100 kHz (same as that of SOI's symbol rate). The frequency offsets of the tones with respect to the carrier in Fig.

5(c) are 100kHz, -300kHz , 0Hz, 400kHz and -100kHz , respectively, and their DOAs are 30° , -50° , -20° , 19° and 45° . In Fig. 5(d), there is one incident MAI signal with three-ray multipath delays of 3 chips, 5 chips and 4 chips arriving from 30° , -20° and -50° , respectively. We can see that the theoretical values of $G(\text{SNR})$ match with the simulated ones very well.

To verify the validity of the approximation given by Lemma 4, in Fig. 6(a) and Fig. 6(b), we also show the curves of $\gamma_0 + 1$, $\gamma_1 + 1$, and λ_{\max} . We can see that $\max\{\gamma_0 + 1, \gamma_1 + 1\}$ can be an excellent approximation for λ_{\max} . In Fig. 7(a) and Fig. 7(b), we show the array patterns that are below and above the threshold. The results in these four figures are simulated under two periodical noises, with the same parameter as Fig. 5(b). The case for the tone jammers and the multiple access interference cases are quite similar, and is thus omitted.

For the Maximin algorithm, all the curves of $G(\text{SNR})$ have failure area, threshold area and operating area, which are consistent with the typical curve in Fig. 2(a). We have also marked the predicted thresholds of SNR_{T1} and SNR_{T2} , computed by (22), in the figures as well, which confirm our theoretical calculations. Furthermore, they also show that the threshold SNR would increase with the interference INR. This is because $\gamma_1 + 1$ (c.f. Fig. 6(a)) would moving upward as INR increases, making the intersecting point of $\gamma_0 + 1$ and $\gamma_1 + 1$ move rightwards. This is consistent with our claim in Section IV-B2 that γ_1 would increase unboundedly with the INR. Fig. 7(a) and Fig. 7(b) show its array pattern below and above threshold, respectively. We can see that the mainlobe of the beamformer would mistakenly point to the interferers once the SNR is below the threshold, as we have predicted in Section III-C.

For the PAPC algorithm, Fig. 5(b)–Fig. 5(d) show that there are only failure areas. This is because, no matter how large SNR is, $\gamma_0 + 1$ will never exceeds $\gamma_1 + 1$, as shown by Fig. 6(b). Therefore, the threshold of PAPC in this case is infinity. The array pattern shown in Fig. 7(a) also indicates that its mainlobe has pointed to the interferers. We have stated in section III-C that the presence of SOI in $\mathbf{R}_{\mathcal{I}}$ will make the beamformer mistakenly null the SOI. The curves of PAPC in Fig. 5(b)–Fig. 5(d) confirms this observation, and Fig. 7(b) shows that PAPC beamformer has a deep null in the direction of the SOI.

In summary, the conventional MPB like Maximin and PAPC work well in the presence of directional white noise, even when the INR is large. However, they are very vulnerable to multiple directional periodical interferers with repeating structures in the time domain and arrive from different directions.

VI. CONCLUSIONS

Matrix pair beamformer (MPB) is a general framework we proposed to model a class of blind beamformers that exploit the temporal signature of the signal of interest (SOI). It has the advantages

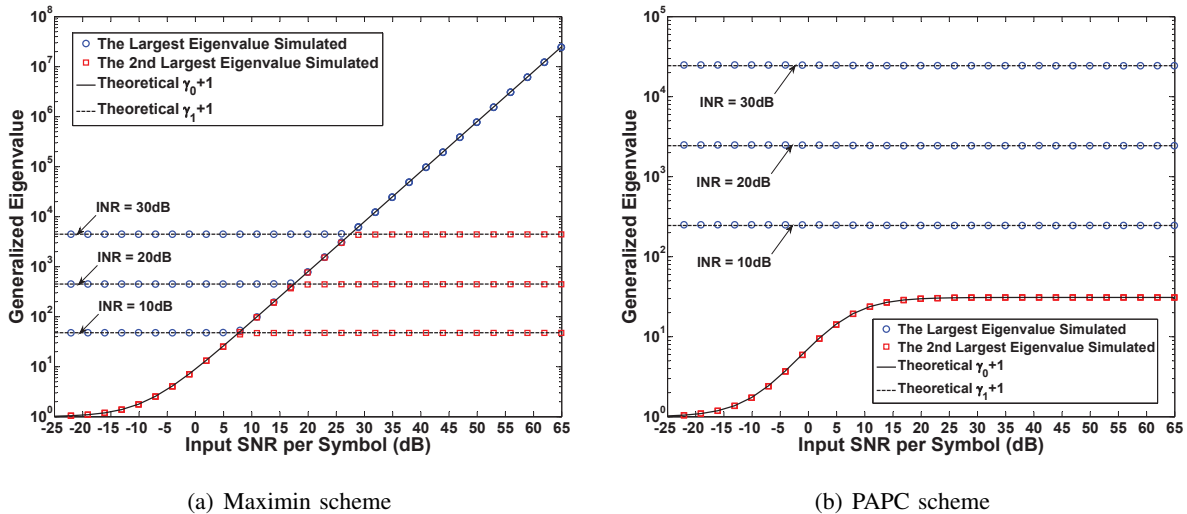


Fig. 6. The largest and second largest generalized eigenvalues of the Maximin scheme vs SNR under two periodical noises.

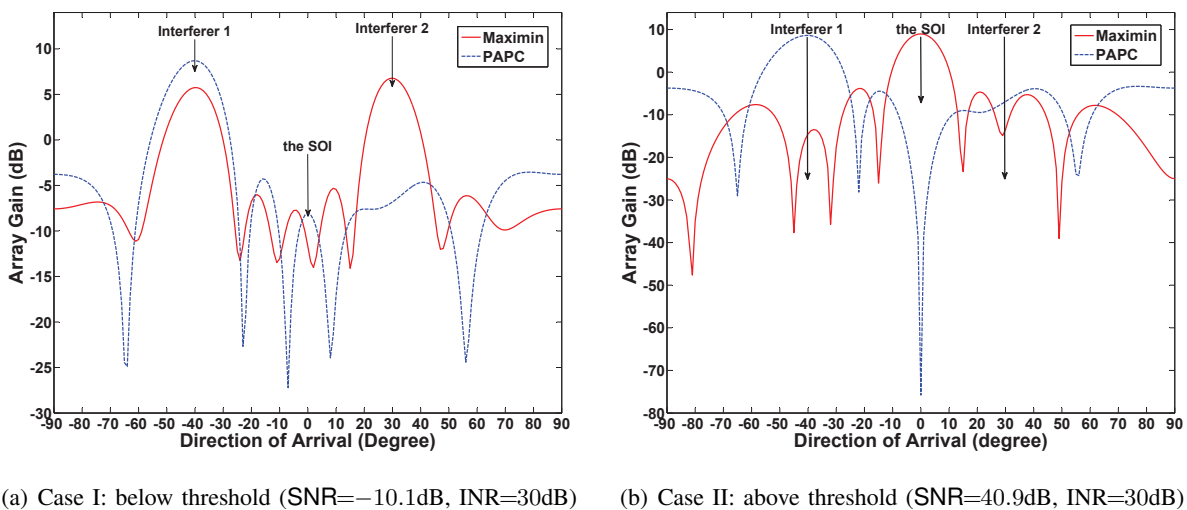


Fig. 7. The array patterns corresponding to the Maximin and PAPC under two periodical noises.

only relying on the second order statistics to achieve blind processing. In this paper, we have analyzed the mechanism of MPB with matrix mismatch, and showed how it worked “blindly”. We have discovered that there is a threshold effect in MPB, i.e. the beamformer would fail completely if the SOI’s input SNR is below that threshold. Meanwhile, its normalized output SINR has been derived as the performance measure, and the threshold SNR has also been predicted. We have also observed that the existence of infinite generalized eigenvalue in what is called *noise free pair* makes the threshold increase unboundedly with the interference power. This is highly probable when there are multiple periodical interferers. All

our theoretical analysis matches with the simulation results very well.

Our analysis indicates that the conventional MPB is very vulnerable to multiple periodical interferers. Moreover, it also implies the importance of choosing the appropriate projection space for the interference channel. And we will address this issue in another paper [36].

APPENDIX A

APPROXIMATION OF λ_{\max} AND γ_i

A. Approximation of λ_{\max}

Since similarity transform does not change the eigenvalues, we can apply it to \mathbf{M} before using Lemma 2. As we will see later, the bounds derived in this way can be surprisingly tight. Though any transform matrix can be used, we prefer the following diagonal matrix that can preserve the diagonal terms of \mathbf{M}

$$\mathbf{F} = \text{diag}\{1, f_1, f_2, \dots, f_D\}, \quad (f_i > 0, i = 1, 2, \dots, D)$$

Applying it to \mathbf{M} in (31) and using Lemma 2, we can have the following Gerschgorin disks for $\mathbf{F}\mathbf{M}\mathbf{F}^{-1}$:

$$G_i = \{\lambda : |\lambda - (\gamma_i + 1)| < R_i(\mathbf{F})\}, \quad i = 0, 1, 2, \dots, D,$$

where the radii of the disks are

$$R_0(\mathbf{F}) = \gamma_0 \sqrt{\frac{\sigma^2}{L}} \sum_{i=1}^D |\psi_{T_i}| \frac{1}{f_i} \quad (49)$$

$$R_i(\mathbf{F}) = \gamma_i \frac{\sqrt{\frac{\sigma^2}{L}} |\psi_{T_i}| \cdot \text{sgn}(\gamma_i)}{\frac{L\beta}{N} \text{SNR} + 1} f_i, \quad 1 \leq i \leq D, \quad (50)$$

with ψ_{T_i} being the i th component of $\boldsymbol{\psi}_T$. Now, we are going to optimize f_1, \dots, f_D . To derive an effective bound for λ_{\max} , we should ensure the rightmost disk is separated from the others (c.f. Lemma 2). Therefore, our criterion for finding the optimal \mathbf{F} is *minimizing the radius of the rightmost Gerschgorin disk subject to the constraint that it is separated from all the remaining ones*. Depending on $\gamma_0 + 1 > \gamma_1 + 1$ or $\gamma_0 + 1 < \gamma_1 + 1$, the rightmost disk might be G_0 or G_1 , and we now discuss them separately.

If $\gamma_0 + 1 > \gamma_1 + 1$, then G_0 is the rightmost disk, and we can formulate the optimization of \mathbf{F} as

$$\min R_0(\mathbf{F}) = \gamma_0 \sqrt{\frac{\sigma^2}{L}} \sum_{i=1}^D |\psi_{T_i}| \frac{1}{f_i} \quad (51)$$

$$\text{s.t. } \gamma_i + 1 + R_i(\mathbf{F}) \leq \gamma_0 + 1 - R_0(\mathbf{F}), \quad 1 \leq i \leq D. \quad (52)$$

To minimize $R_0(\mathbf{F})$, we want f_1, \dots, f_D to be as large as possible. But this will increase the radius of G_1, \dots, G_D , and to avoid connecting G_0 , they cannot be too large. In fact, f_1, \dots, f_D have different

importance in this tradeoff. Since $\gamma_0 > \dots > \gamma_D$, G_2, \dots, G_D are farther away from G_0 than G_1 . Therefore, f_2, \dots, f_D can be reasonably larger than f_1 when keeping separate from G_0 . Thus, to simplify analysis, we can ignore all the terms except $|\psi_{T_1}|/f_1$ in $R_0(\mathbf{F})$, i.e. $R_0(\mathbf{F}) \approx \gamma_0 \sqrt{\frac{\sigma^2}{L}} \frac{|\psi_{T_1}|}{f_1}$ in (51) and (52), and only the constraint for $i = 1$ is effective in (52). Then, the problem can be reduced to

$$\begin{aligned} \min \quad & R_0(\mathbf{F}) \approx \gamma_0 \sqrt{\frac{\sigma^2}{L}} |\psi_{T_1}| \frac{1}{f_1} \\ \text{s.t.} \quad & \gamma_1 \frac{\sqrt{\frac{\sigma^2}{L}} |\psi_{T_1}| \cdot \text{sgn}(\gamma_1)}{\frac{L\beta}{N} \text{SNR} + 1} f_1^2 - (\gamma_0 - \gamma_1) f_1 + \gamma_0 \sqrt{\frac{\sigma^2}{L}} |\psi_{T_1}| \leq 0. \end{aligned}$$

This is a simple convex optimization problem, feasible when $\frac{\gamma_1}{\gamma_0} \in (-\infty, 1 + 2\delta - \sqrt{(1 + 2\delta)^2 - 1}]$, where $\delta \triangleq \frac{\sigma^2}{L} |\psi_{T_1}|^2 / (\frac{L\beta}{N} \text{SNR} + 1) \ll 1$. Thus, we can easily solve the above optimization and get

$$|\lambda_{\max} - (\gamma_0 + 1)| < \gamma_0 \cdot f \left(\frac{\gamma_1}{\gamma_0} \right)$$

where $f(x) \triangleq \frac{1}{2} [1 - x - \sqrt{(1-x)^2 - 4\delta|x|}]$ with $x \in (-\infty, 1 - 2\sqrt{\delta + \delta^2} + 2\delta] \cup [1 + 2\sqrt{\delta + \delta^2} + 2\delta, +\infty)$. Furthermore, by taking the derivative of $f(x)$, we can easily get $0 \leq f(x) \leq \max\{\delta, \sqrt{\delta^2 + \delta} - \delta\} \ll 1$ when $x \in (-\infty, 1 - 2\sqrt{\delta + \delta^2} + 2\delta]$.

If $\gamma_0 + 1 < \gamma_1 + 1$, then G_1 is the rightmost disk and $\gamma_1 > 0$. The optimization problem is

$$\min \quad R_1(\mathbf{F}) = \gamma_1 \frac{\sqrt{\frac{\sigma^2}{L}} |\psi_{T_1}|}{\frac{L\beta}{N} \text{SNR} + 1} f_1 \quad (53)$$

$$\text{s.t.} \quad \gamma_0 + 1 + R_0(F) \leq \gamma_1 + 1 - R_1(\mathbf{F}), \quad (54)$$

$$\gamma_i + 1 + R_i(F) \leq \gamma_1 + 1 - R_1(\mathbf{F}), \quad 2 \leq i \leq D. \quad (55)$$

According to (49) and (50), f_1 should be as small as possible to minimize $R_1(\mathbf{F})$ in (53), (54) and (55). However, this will increase $R_0(\mathbf{F})$ in (54), making G_0 connect with G_1 . Therefore, f_1 cannot be arbitrarily small. On the other hand, f_2, \dots, f_D should be as large as possible to reduce $R_0(\mathbf{F})$ in (54) while keeping (55) valid. As a result, $|\psi_{T_1}|/f_1$ is still the dominant term in $R_0(\mathbf{F})$ (c.f. (49)) and the key point here remains the tradeoff between $R_1(\mathbf{F})$ and $R_0(\mathbf{F})$. In other words, the optimization becomes

$$\begin{aligned} \min \quad & R_1(\mathbf{F}) = \gamma_1 \frac{\sqrt{\frac{\sigma^2}{L}} |\psi_{T_1}|}{\frac{L\beta}{N} \text{SNR} + 1} f_1 \\ \text{s.t.} \quad & \gamma_1 \frac{\sqrt{\frac{\sigma^2}{L}} |\psi_{T_1}|}{\frac{L\beta}{N} \text{SNR} + 1} f_1^2 - (\gamma_1 - \gamma_0) f_1 + \gamma_0 \sqrt{\frac{\sigma^2}{L}} |\psi_{T_1}| \leq 0. \end{aligned}$$

The feasible region for this convex optimization is $\frac{\gamma_1}{\gamma_0} \in [1 + 2\delta + \sqrt{(1 + 2\delta)^2 - 1}, +\infty)$, with δ defined in the previous case. By solving it, we can finally get the bound for λ_{\max} as

$$|\lambda_{\max} - (\gamma_1 + 1)| \leq \gamma_1 \cdot f\left(\frac{\gamma_0}{\gamma_1}\right)$$

where $f(x)$ is the same as in the previous case.

B. Approximation of γ_i

Then, we discuss the approximation of γ_i . By substituting (5) into (28) and using matrix inversion lemma, we can have the equivalent equation of (28) as

$$\det(\mathbf{A}_I^H \mathbf{R}_{\mathcal{I}}^{-1} \mathbf{A}_I)^{-1} \cdot \det \left\{ \lambda \mathbf{I} - \left[\mathbf{A}_I^H \mathbf{Q}_{\mathcal{I}}^{-1} \mathbf{A}_I - \frac{\sigma_{\mathcal{I}}^2 \mathbf{A}_I^H \mathbf{Q}_{\mathcal{I}}^{-1} \mathbf{a}_0 \cdot \mathbf{a}_0^H \mathbf{Q}_{\mathcal{I}}^{-1} \mathbf{A}_I}{1 + \sigma_{\mathcal{I}}^2 \mathbf{a}_0^H \mathbf{Q}_{\mathcal{I}}^{-1} \mathbf{a}_0} \right] \Phi_{\Delta} \right\} = 0 \quad (56)$$

To further reduce the above expression, we need factorizations of $\mathbf{A}_I^H \mathbf{Q}_{\mathcal{I}}^{-1} \mathbf{A}_I$ and Φ_{Δ} like (26). Let $\sigma_{\mathcal{I}_0}^2 = 0$ in (26). Then, $\mathbf{R}_{\mathcal{I}} = \mathbf{Q}_{\mathcal{I}}$, and (26) become

$$\mathbf{T}_0^H \Phi_{\Delta} \mathbf{T}_0 = \mathbf{\Gamma}_0, \quad \mathbf{T}_0^H (\mathbf{A}_I^H \mathbf{Q}_{\mathcal{I}}^{-1} \mathbf{A}_I)^{-1} \mathbf{T}_0 = \mathbf{I}.$$

where \mathbf{T}_0 and $\mathbf{\Gamma}_0$ are the counterparts of \mathbf{T} and $\mathbf{\Gamma}$, respectively. Substituting them into (56), we have

$$\det(\mathbf{A}_I^H \mathbf{R}_{\mathcal{I}}^{-1} \mathbf{A}_I)^{-1} \cdot \det \left\{ \lambda \mathbf{I} - \left[\mathbf{I} - \frac{\sigma_{\mathcal{I}}^2 \tilde{\psi}_{T_0} \tilde{\psi}_{T_0}^H}{1 + \sigma_{\mathcal{I}}^2 \mathbf{a}_0^H \mathbf{Q}_{\mathcal{I}}^{-1} \mathbf{a}_0} \right] \mathbf{\Gamma}_0 \right\} = 0$$

where $\tilde{\psi}_{T_0} = \mathbf{T}_0^{-1} \mathbf{A}_I^H \mathbf{Q}_{\mathcal{I}}^{-1} \mathbf{a}_0$ is the counterpart of $\tilde{\psi}_T$ when $\sigma_{\mathcal{I}_0}^2 = 0$. By letting $\text{SNR} = 0$ in Lemma 1, $\mathbf{R}_{\mathcal{I}}$ becomes $\mathbf{Q}_{\mathcal{I}}$ and we can have $\mathbf{a}_0^H \mathbf{Q}_{\mathcal{I}}^{-1} \mathbf{a}_0 \approx L/\sigma^2$ and $\|\tilde{\psi}_{T_0}\|^2 = L\kappa_0/\sigma^2 \ll L/\sigma^2$. Therefore, by the similar argument of λ_{\max} using Gerschgorin theorem, we can have $\gamma_i \approx \lambda_{i,0}$, where $\lambda_{i,0}$ is the i th diagonal term of $\mathbf{\Gamma}_0$, namely, the i th eigenvalue of $(\Phi_{\Delta}, (\mathbf{A}_I^H \mathbf{Q}_{\mathcal{I}}^{-1} \mathbf{A}_I)^{-1})$. In fact, there is a correspondence between $\lambda_{i,0}$ and the generalized eigenvalue of $(\mathbf{Q}_S - \mathbf{Q}_{\mathcal{I}}, \mathbf{Q}_{\mathcal{I}})$. By (29),

$$\det \{ \lambda (\mathbf{A}_I^H \mathbf{Q}_{\mathcal{I}}^{-1} \mathbf{A}_I)^{-1} - \Phi_{\Delta} \} = \lambda^{D-L} \cdot \det(\mathbf{A}_I^H \mathbf{Q}_{\mathcal{I}}^{-1} \mathbf{A}_I)^{-1} \det \mathbf{Q}_{\mathcal{I}}^{-1} \cdot \det \{ \lambda \mathbf{Q}_{\mathcal{I}} - \mathbf{A}_I \Phi_{\Delta} \mathbf{A}_I^H \}.$$

Since $\mathbf{Q}_S - \mathbf{Q}_{\mathcal{I}} = \mathbf{A}_I \Phi_{\Delta} \mathbf{A}_I^H$, the above expression implies that $(\Phi_{\Delta}, (\mathbf{A}_I^H \mathbf{Q}_{\mathcal{I}}^{-1} \mathbf{A}_I)^{-1})$ has the same eigenvalues as $(\mathbf{Q}_S - \mathbf{Q}_{\mathcal{I}}, \mathbf{Q}_{\mathcal{I}})$ except for multiplicity of zeros. Thus, we can estimate γ_i like this: 1) take out all nonzero eigenvalues of $(\mathbf{Q}_S - \mathbf{Q}_{\mathcal{I}}, \mathbf{Q}_{\mathcal{I}})$, 2) pad them up to D eigenvalues with zeros, 3) order them decreasingly to get $\lambda_{1,0}, \dots, \lambda_{D,0}$, and 4) let $\gamma_i \approx \lambda_{i,0}$.

APPENDIX B

PROOF OF LEMMA 3

Substituting the definitions of $y_S(k)$ and $y_I(k)$ (c.f. (10)), (6) and (14) into (17), we can have

$$\mathsf{G}(\text{SNR}) = \frac{|\mathbf{w}^H \mathbf{a}_0|^2}{\mathbf{w}^H \mathbf{A}_I \Phi_S \mathbf{A}_I^H \mathbf{w} + \sigma^2 \|\mathbf{w}\|^2} \frac{1}{\mathbf{a}_0^H \mathbf{Q}_S^{-1} \mathbf{a}_0} \approx \frac{|\mathbf{w}^H \mathbf{a}_0|^2}{\mathbf{w}^H \mathbf{A}_I \Phi_S \mathbf{A}_I^H \mathbf{w} + \sigma^2 \|\mathbf{w}\|^2} \frac{L}{\sigma^2}, \quad (57)$$

where we used $\mathbf{a}_0^H \mathbf{Q}_S^{-1} \mathbf{a}_0 \approx L/\sigma^2$, derived by replacing \mathbf{R}_I with \mathbf{R}_S and letting $\sigma_{S_0}^2=0$ in Lemma 1.

To further derive G , we first need the expression for $\|\mathbf{w}\|^2$. The key trick is to recognize that $\mathbf{w} \in \mathcal{R}(\mathbf{A})$ so that its projection onto $\mathcal{R}(\mathbf{A})$ equals itself, where $\mathcal{R}(\cdot)$ is the range space of a matrix and $\mathbf{A} \triangleq [\mathbf{a}_0 \ \mathbf{A}_I]$. This can be proved by substituting (7) into (5), applying matrix inversion lemma and plugging it into (25). Furthermore, $\mathcal{R}(\mathbf{A}_I)$ is a subspace of $\mathcal{R}(\mathbf{A})$ with the dimension lower by one. Thus, $\mathcal{R}(\mathbf{A}) = \mathcal{R}(\mathbf{A}) \oplus \mathcal{R}(\hat{\mathbf{b}}_0)$, where \oplus denotes the direct sum and $\hat{\mathbf{b}}_0$ is the unit vector in $\mathcal{R}(\mathbf{A})$ that is orthogonal to $\mathcal{R}(\mathbf{A}_I)$. Then, the projection matrix of $\mathcal{R}(\mathbf{A})$ can be written as

$$\mathbf{P}_A = \mathbf{A}_I (\mathbf{A}_I^H \mathbf{A}_I)^{-1} \mathbf{A}_I^H + \hat{\mathbf{b}}_0 \hat{\mathbf{b}}_0^H.$$

This together with $\mathbf{P}_A \mathbf{w} = \mathbf{w}$ and $\mathbf{P}_A^2 = \mathbf{P}_A$ yields

$$\|\mathbf{w}\|^2 = \mathbf{w}^H \mathbf{P}_A \mathbf{w} = \mathbf{w}^H \mathbf{A}_I (\mathbf{A}_I^H \mathbf{A}_I)^{-1} \mathbf{A}_I^H \mathbf{w} + |\mathbf{w}^H \hat{\mathbf{b}}_0|^2 \quad (58)$$

Assumption 1 in Sec. III-A implies that \mathbf{a}_0 is almost orthogonal to $\mathcal{R}(\mathbf{A}_I)$. Thus, it is nearly aligned with $\hat{\mathbf{b}}_0$, and intuitively, $|\mathbf{w}^H \hat{\mathbf{b}}_0| \approx |\mathbf{w}^H \hat{\mathbf{a}}_0|$, where $\hat{\mathbf{a}}_0 \triangleq \mathbf{a}_0 / \|\mathbf{a}_0\|$ is the unit vector of \mathbf{a}_0 . To prove it, let $\mathcal{R}_0 \triangleq \text{span}\{\hat{\mathbf{a}}_0, \hat{\mathbf{b}}_0\}$ and $\{\hat{\mathbf{b}}_0, \hat{\mathbf{b}}_1\}$ be the orthonormal basis of \mathcal{R}_0 . Its projection matrix becomes $\mathbf{P}_{\mathcal{R}_0} = \hat{\mathbf{b}}_0 \hat{\mathbf{b}}_0^H + \hat{\mathbf{b}}_1 \hat{\mathbf{b}}_1^H$, which satisfies $\mathbf{P}_{\mathcal{R}_0} \hat{\mathbf{a}}_0 = \hat{\mathbf{a}}_0$ and $\mathbf{P}_{\mathcal{R}_0} \hat{\mathbf{b}}_0 = \hat{\mathbf{b}}_0$. Define $\mathbf{w}_0 = \mathbf{P}_{\mathcal{R}_0} \mathbf{w} / \|\mathbf{P}_{\mathcal{R}_0} \mathbf{w}\|$. Then,

$$\begin{aligned} |\mathbf{w}^H \hat{\mathbf{b}}_0|^2 &= |\mathbf{w}^H \hat{\mathbf{a}}_0|^2 + [|\mathbf{w}^H \hat{\mathbf{b}}_0|^2 - |\mathbf{w}^H \hat{\mathbf{a}}_0|^2] = |\mathbf{w}^H \hat{\mathbf{a}}_0|^2 + [|\mathbf{w}^H \mathbf{P}_{\mathcal{R}_0} \hat{\mathbf{b}}_0|^2 - |\mathbf{w}^H \mathbf{P}_{\mathcal{R}_0} \mathbf{P}_{\mathcal{R}_0} \hat{\mathbf{a}}_0|^2] \\ &= |\mathbf{w}^H \hat{\mathbf{a}}_0|^2 + \|\mathbf{P}_{\mathcal{R}_0} \mathbf{w}\|^2 [|\mathbf{w}_0^H \hat{\mathbf{b}}_0|^2 - |\mathbf{w}_0^H \hat{\mathbf{b}}_0 \cdot \hat{\mathbf{b}}_0^H \hat{\mathbf{a}}_0 + \mathbf{w}_0^H \hat{\mathbf{b}}_1 \cdot \hat{\mathbf{b}}_1^H \hat{\mathbf{a}}_0|^2] \\ &= |\mathbf{w}^H \hat{\mathbf{a}}_0|^2 + \|\mathbf{P}_{\mathcal{R}_0} \mathbf{w}\|^2 \cdot \cos \phi_I \cdot \cos(\phi_1 + 2\phi_I) \end{aligned} \quad (59)$$

where ϕ_I is the angle between $\hat{\mathbf{a}}_0$ and $\mathcal{R}(\mathbf{A}_I)$, and ϕ_1 is the angle between $\hat{\mathbf{a}}_0$ and $\hat{\mathbf{b}}_0$. And the derivation of the last step in (59) involves some simple trigonometry identities like product-to-sum formula. Let $\Psi_I \triangleq \mathbf{A}_I^H \mathbf{A}_I / L$. Combining (58), (59), $\|\mathbf{P}_{\mathcal{R}_0} \mathbf{w}\| \leq \|\mathbf{w}\|$ and $|\cos \phi_I| \ll 1$ (c.f. Assumption 1), we can have

$$\|\mathbf{w}\|^2 = \frac{\frac{1}{L} [|\mathbf{a}_0^H \mathbf{w}|^2 + \mathbf{w}^H \mathbf{A}_I \Psi_I^{-1} \mathbf{A}_I^H \mathbf{w}]}{1 - \frac{\|\mathbf{P}_{\mathcal{R}_0} \mathbf{w}\|^2}{\|\mathbf{w}\|^2} \cdot \cos \phi_I \cdot \cos(\phi_1 + 2\phi_I)} \approx \frac{1}{L} [|\mathbf{a}_0^H \mathbf{w}|^2 + \mathbf{w}^H \mathbf{A}_I \Psi_I^{-1} \mathbf{A}_I^H \mathbf{w}],$$

where we also used $\|\mathbf{a}_0\|^2 = L$ in Assumption 2. Substitute the above expression back to (57), and we get

$$\mathsf{G}(\text{SNR}) \approx \frac{|\mathbf{w}^H \mathbf{a}_0|^2}{\mathbf{w}^H \mathbf{A}_I \left[\frac{L}{\sigma^2} \Phi_S + \Psi_I^{-1} \right] \mathbf{A}_I^H \mathbf{w} + |\mathbf{w}^H \mathbf{a}_0|^2}. \quad (60)$$

Next, we are going to evaluate $\mathbf{w}^H \mathbf{a}_0$ and $\mathbf{w}^H \mathbf{A}_I [\frac{L}{\sigma^2} \Phi_S + \Psi_I^{-1}] \mathbf{A}_I^H \mathbf{w}$. By the expression of \mathbf{w} in (25),

$$\begin{aligned} \mathbf{a}_0^H \mathbf{w} &= \mathbf{a}_0^H \mathbf{R}_{\mathcal{I}}^{-1} \mathbf{a}_0 + \sum_{i=1}^D \frac{\gamma_i}{\lambda_{\max} - (\gamma_i + 1)} |\tilde{\psi}_{T_i}|^2 = \mathbf{a}_0^H \mathbf{R}_{\mathcal{I}}^{-1} \mathbf{a}_0 - \|\tilde{\boldsymbol{\psi}}_T\|^2 + \sum_{i=1}^D \frac{\lambda_{\max} - 1}{\lambda_{\max} - (\gamma_i + 1)} |\tilde{\psi}_{T_i}|^2 \\ &\approx \frac{L}{\sigma^2} \left(\frac{L\beta}{N} \text{SNR} + 1 \right) \left[1 + \left(\frac{L\beta}{N} \text{SNR} + 1 \right)^{-1} \psi_S(\lambda_{\max}) \right], \end{aligned} \quad (61)$$

where we used Lemma 1 in the approximation and $\psi_S(\lambda_{\max})$ is defined as (37) in Lemma 3. Before the derivation of $\mathbf{w}^H \mathbf{A}_I [\frac{L}{\sigma^2} \Phi_S + \Psi_I^{-1}] \mathbf{A}_I^H \mathbf{w}$, we first cite the following identity from Lemma 2 in [35].

$$\frac{L}{\sigma^2} \Phi_{\mathcal{I}} + \Psi_I^{-1} = \frac{L}{\sigma^2} (\mathbf{T}^{-1})^H \left[\mathbf{I} - \frac{L\beta \text{SNR} \cdot \frac{\sigma^2}{L} \boldsymbol{\psi}_T \boldsymbol{\psi}_T^H}{L\beta(1-\rho_0)\text{SNR} + N} \right] \mathbf{T}^{-1}.$$

Then, combining the above expression together with $\Phi_{\Delta} = \Phi_S - \Phi_{\mathcal{I}}$, (26) and $\mathbf{A}_{\epsilon} \triangleq \mathbf{A}_I (\mathbf{T}^{-1})^H$ we can have

$$\begin{aligned} \mathbf{w}^H \mathbf{A}_I \left[\frac{L}{\sigma^2} \Phi_S + \Psi_I^{-1} \right] \mathbf{A}_I^H \mathbf{w} &= \frac{L}{\sigma^2} \mathbf{w}^H \mathbf{A}_I (\mathbf{T}^{-1})^H \left[\mathbf{I} + \boldsymbol{\Gamma} - \frac{L\beta \text{SNR} \cdot \frac{\sigma^2}{L} \boldsymbol{\psi}_T \boldsymbol{\psi}_T^H}{L\beta(1-\rho_0)\text{SNR} + N} \right] \mathbf{T}^{-1} \mathbf{A}_I^H \mathbf{w} \\ &\approx \left[\frac{NL/\sigma^2}{L\beta \text{SNR} + N} \right]^2 \left[\psi_I(\lambda_{\max}) - \frac{L\beta \text{SNR}}{L\beta \text{SNR} + N} \psi_S^2(\lambda_{\max}) \right], \end{aligned} \quad (62)$$

where $\psi_I(\lambda_{\max})$ is also given by (37) in Lemma 3, and $\rho_0 \ll 1$ is a small number independent of SNR.

Finally, substituting (61) and (62) into (60), we can derive $\mathbf{G}(\text{SNR})$ in (36) immediately.

REFERENCES

- [1] P. Howells, "Intermediate frequency side-lobe canceller," Patent, 1965, US Patent 3,202,990.
- [2] S. Applebaum, "Adaptive arrays," *IEEE Trans. Antennas Propag.*, vol. 24, no. 5, pp. 585–598, 1976.
- [3] B. Widrow, P. Mantey, L. Griffiths, and B. Goode, "Adaptive antenna systems," *Proc. IEEE*, vol. 55, no. 12, pp. 2143–2159, 1967.
- [4] B. Widrow, J. Glover Jr, J. McCool, J. Kaunitz, C. Williams, R. Hearn, J. Zeidler, E. Dong Jr, and R. Goodlin, "Adaptive noise cancelling: Principles and applications," *Proc. IEEE*, vol. 63, no. 12, pp. 1692–1716, 1975.
- [5] W. Gabriel, "Adaptive arrays: An introduction," *Proc. IEEE*, vol. 64, no. 2, pp. 239–272, 1976.
- [6] J. Compton, R.T., "An adaptive array in a spread-spectrum communication system," *Proc. IEEE*, vol. 66, no. 3, pp. 289–298, 1978.
- [7] R. Compton Jr, R. Huff, and W. Swarner, "Adaptive Arrays for Communication Systems: An Overview of Research at The Ohio State University," *IEEE Trans. Antennas Propag.*, vol. 24, no. 5, pp. 599–607, 1976.
- [8] S. Haykin, "Array processing—Applications to radar," *NASA STI/Recon Technical Report A*, vol. 80, 1980.
- [9] L. Godara, "Application of Antenna Arrays to Mobile Communications. Part I: Performance Improvement, Feasibility and System Considerations," *Proc. IEEE*, vol. 85, no. 7, pp. 1031–1060, 1997.
- [10] —, "Application of antenna arrays to mobile communications. II. Beam-forming and direction-of-arrival considerations," *Proc. IEEE*, vol. 85, no. 8, pp. 1195–1245, 1997.

- [11] A. Paulraj and C. Papadias, "Space-time processing for wireless communications," *IEEE Signal Process. Mag.*, vol. 14, no. 6, pp. 49–83, 1997.
- [12] B. Van Veen and K. Buckley, "Beamforming: a versatile approach to spatial filtering," *IEEE ASSP Mag.*, vol. 5, no. 2, pp. 4–24, 1988.
- [13] S. Haykin and A. Steinhardt, "Adaptive radar detection and estimation," New York: John Wiley & Sons, Inc., 1992.
- [14] H. Krim and M. Viberg, "Two decades of array signal processing research: the parametric approach," *IEEE Signal Process. Mag.*, vol. 13, no. 4, pp. 67–94, 1996.
- [15] H. L. Van Trees, *Optimum Array Processing—Part IV of Detection, Estimation and Modulation Theory*. New York: John Wiley & Sons, Inc., 2002.
- [16] I. Reed, J. Mallett, and L. Brennan, "Rapid Convergence Rate in Adaptive Arrays," *IEEE Trans. Aerosp. Electron. Syst.*, vol. AES-10, no. 6, pp. 853–863, 1974.
- [17] S. Tanaka, A. Harada, M. Sawahashi, and F. Adachi, "Experiments on coherent adaptive antenna array diversity for wideband DS-CDMA mobile radio," *IEEE J. Sel. Areas Comm.*, vol. 18, no. 8, pp. 1495–1504, 2000.
- [18] D. Godard, "Self-recovering equalization and carrier tracking in two-dimensional data communication systems," *IEEE Trans. Comm.*, vol. 28, no. 11, pp. 1867–1875, 1980.
- [19] J. Treichler and B. Agee, "A new approach to multipath correction of constant modulus signals," *IEEE Trans. Acoust., Speech, Signal Process.*, vol. 31, no. 2, pp. 459–472, 1983.
- [20] J. Shynk and C. Chan, "Performance surfaces of the constant modulus algorithm based on a conditional Gaussian model," *IEEE Trans. Signal Process.*, vol. 41, no. 5, pp. 1965–1969, 1993.
- [21] T. Ohgane, "Characteristics of CMA adaptive array for selective fading compensation in digital land mobile radio communications," *Electronics and Communications in Japan (Part I: Communications)*, vol. 74, no. 9, pp. 43–53, 1991.
- [22] T. Ohgane, T. Shimura, N. Matsuzawa, and H. Sasaoka, "An implementation of a CMA adaptive array for high speed GMSK transmission in mobile communications," *IEEE Trans. Veh. Technol.*, vol. 42, no. 3, pp. 282–288, 1993.
- [23] A. F. Naguib, "Adaptive Antennas for CDMA Wireless Networks," Ph.D. Dissertation, Stanford University, August 1996.
- [24] B. Suard, A. Naguib, G. Xu, and A. Paulraj, "Performance of CDMA mobile communication systems using antenna arrays," *IEEE International Conference on Acoustics, Speech, and Signal Processing*, vol. 4, pp. 153–156, 1993.
- [25] S. Choi, J. Choi, H. Im, and B. Choi, "A Novel Adaptive Beamforming Algorithm for Antenna Array CDMA Systems With Strong Interferers," in *IEEE Trans. Veh. Technol.*, vol. 51, no. 5, pp. 808–816, 2002.
- [26] J. Yang, H. Xi, F. Yang, and Y. Zhao, "Fast adaptive blind beamforming algorithm for antenna array in CDMA systems," *IEEE Trans. Veh. Technol.*, vol. 55, no. 2, pp. 549–558, 2006.
- [27] Y. Song, H. Kwon, and B. Min, "Computationally efficient smart antennas for CDMA wireless communications," *IEEE Trans. Veh. Technol.*, vol. 50, no. 6, pp. 1613–1628, 2001.
- [28] D. Torrieri and K. Bakhru, "A direct-sequence adaptive array," in *IEEE Military Communications Conference*, vol. 3, 2004, pp. 1444–1450.
- [29] —, "The Maximin Adaptive-Array Algorithm for Direct-Sequence Systems," *IEEE Trans. Signal Process.*, vol. 55, no. 5 Part 1, pp. 1853–1861, 2007.
- [30] J. Chen, J. Wang, P. Zhang, J. Yuan, and X. Shan, "An Orthogonal Projection Approach for Blind Beamforming in Multipath CDMA Channels," in *6th Annual Communication Networks and Services Research Conference*, 2008, pp. 496–503.
- [31] —, "An Orthogonal Projection Based Blind Beamformer for DS-CDMA Systems," in *5th IEEE Sensor Array and Multichannel Signal Processing Workshop*, 2008, pp. 37–40.

- [32] G. Stewart and J. Sun, *Matrix perturbation theory (Computer science and scientific computing)*. Academic Press, 1990.
- [33] R. Horn and C. Johnson, *Matrix analysis*. Cambridge University Press, 1990.
- [34] A. Laub, *Matrix analysis for scientists & engineers*. Society for Industrial and Applied Mathematics, 2004.
- [35] J. Chen and J. Wang, "Some Fundamental Results of Matrix for the Paper: Performance Analysis of the Matrix Pair Beamformer with Matrix Mismatch." [Online]. Available: <http://arxiv.org/abs/1009.5979>
- [36] J. Wang, J. Chen, J. Yuan, N. Ge, and S. Wei, "An Adaptive Beamforming Algorithm for Direct Spread Systems with Mitigated Threshold Effect," *Submitted*.

Some Fundamental Results of Matrix for the Paper “Performance Analysis of the Matrix Pair Beamformer with Matrix Mismatch”

Jianshu Chen, *Student Member, IEEE*, and Jian Wang

Abstract

We give some key results for the paper “Performance Analysis of the Matrix Pair Beamformer with Matrix Mismatch”.

Index Terms

Adaptive beamforming, Matrix pair beamformer, MPB, Generalized eigen-decomposition, Matrix mismatch

I. INTRODUCTION

We give some key results for the paper “Performance Analysis of the Matrix Pair Beamformer with Matrix Mismatch”.

II. PROBLEM FORMULATION

The analysis of the performance of the matrix pair beamformer requires the expression of $\mathbf{A}^H \mathbf{R}_{\mathcal{I}}^{-1} \mathbf{A}$, where

$$\mathbf{R}_{\mathcal{I}} \triangleq \sigma_{I_0}^2 \mathbf{a}_0 \mathbf{a}_0^H + \underbrace{\mathbf{A}_I \Phi_{\mathcal{I}} \mathbf{A}_I^H}_{\mathbf{Q}_{\mathcal{I}}} + \sigma^2 \mathbf{I}, \quad (1)$$

$$\mathbf{A} \triangleq \begin{bmatrix} \mathbf{a}_0 & \mathbf{a}_1 & \cdots & \mathbf{a}_D \end{bmatrix} = \begin{bmatrix} \mathbf{a}_0 & \mathbf{A}_I \end{bmatrix}$$

Jianshu Chen was with the Department of Electronic Engineering, Tsinghua University, Beijing, P. R. China, 100084. He is currently with the Department of Electrical Engineering, University of California, Los Angeles, CA 90095-1594, USA. (e-mail: jshchen@ee.ucla.edu)

Jian Wang, is with the Department of Electronic Engineering, Tsinghua University, Beijing, P. R. China, 100084. (e-mail: jian-wang@tsinghua.edu.cn)

Furthermore, we base our discussion on the following assumptions.

Assumption 1: The spacing of DOA between any two signals is large enough (greater than a mainlobe), so that $\{\mathbf{a}_i\}_{i=0}^D$ is linearly independent and the projection of \mathbf{a}_0 onto $\text{span}\{\mathbf{a}_i\}_{i=1}^D$ is much less than $\|\mathbf{a}_0\|$.

Assumption 2: The steering vector of all signals are normalized so that $\|\mathbf{a}_i\|^2 = L$, ($i = 0, 1, \dots, D$).

III. SOME FUNDAMENTAL RESULTS

The main results are summarized in the following two Lemmas.

Lemma 1: The expression of $\mathbf{A}^H \mathbf{R}_{\mathcal{I}}^{-1} \mathbf{A}$ is given by

$$\mathbf{A}^H \mathbf{R}_{\mathcal{I}}^{-1} \mathbf{A} = \begin{bmatrix} \mathbf{a}_0^H \mathbf{R}_{\mathcal{I}}^{-1} \mathbf{a}_0 & \mathbf{a}_0^H \mathbf{R}_{\mathcal{I}}^{-1} \mathbf{A}_I \\ \mathbf{A}_I^H \mathbf{R}_{\mathcal{I}}^{-1} \mathbf{a}_0 & \mathbf{A}_I^H \mathbf{R}_{\mathcal{I}}^{-1} \mathbf{A}_I \end{bmatrix}$$

where

$$\mathbf{a}_0^H \mathbf{R}_{\mathcal{I}}^{-1} \mathbf{a}_0 = \frac{L}{\sigma^2} \frac{1 - \xi}{\frac{L\beta}{N}(1 - \xi)\text{SNR} + 1} \quad (2)$$

$$\mathbf{A}_I^H \mathbf{R}_{\mathcal{I}}^{-1} \mathbf{a}_0 = \frac{L}{\sigma^2} \frac{1}{\frac{L\beta}{N}(1 - \xi)\text{SNR} + 1} \mathbf{\Xi} \mathbf{\Psi}_I^{-1} \boldsymbol{\psi} \quad (3)$$

$$\mathbf{A}_I^H \mathbf{R}_{\mathcal{I}}^{-1} \mathbf{A}_I = \frac{L}{\sigma^2} \left[\mathbf{\Xi} - \frac{\frac{L\beta}{N}\text{SNR}}{\frac{L\beta}{N}(1 - \xi)\text{SNR} + 1} \mathbf{\Xi} \mathbf{\Psi}_I^{-1} \boldsymbol{\psi} \boldsymbol{\psi}^H \mathbf{\Psi}_I^{-1} \mathbf{\Xi} \right] \quad (4)$$

with $\boldsymbol{\psi} \triangleq \frac{\mathbf{A}_I^H \mathbf{a}_0}{L}$, $\mathbf{\Psi}_I \triangleq \frac{\mathbf{A}_I^H \mathbf{A}_I}{L}$; $\beta = N\sigma_{\mathcal{I}_0}/\sigma_{S_0}$; $\mathbf{\Xi}$ and ξ are defined as

$$\mathbf{\Xi} \triangleq \left[\frac{L}{\sigma^2} \mathbf{S}_{\mathcal{I}} + \mathbf{\Psi}_I^{-1} \right]^{-1}, \quad \xi \triangleq \rho_0 - \kappa_0.$$

$\rho_0 \triangleq \boldsymbol{\psi}^H \mathbf{\Psi}_I^{-1} \boldsymbol{\psi}$ is the projection power of the unit vector of \mathbf{a}_0 onto $\text{span}\{\mathbf{a}_0, \dots, \mathbf{a}_D\}$ and is thus much smaller than 1; $\kappa_0 \triangleq \boldsymbol{\psi}^H \mathbf{\Psi}_I^{-1} \mathbf{\Xi} \mathbf{\Psi}_I^{-1} \boldsymbol{\psi}$. Furthermore, ξ and κ_0 satisfy

$$0 \leq \kappa_0 \leq \rho_0 \ll 1, \quad 0 \leq \xi \leq \rho_0 \ll 1$$

Proof: According to (1), $\mathbf{R}_{\mathcal{I}}$ can be written as

$$\mathbf{R}_{\mathcal{I}} = \mathbf{A} \mathbf{S} \mathbf{A}^H + \sigma^2 \mathbf{I} \quad (5)$$

where \mathbf{A} and \mathbf{S} are defined as

$$\mathbf{A} \triangleq \begin{bmatrix} \mathbf{a}_0 & \mathbf{A}_I \end{bmatrix} \quad (6)$$

$$\mathbf{S} \triangleq \begin{bmatrix} \sigma_{\mathcal{I}_0}^2 & \mathbf{0}^H \\ \mathbf{0} & \mathbf{\Phi}_{\mathcal{I}} \end{bmatrix}. \quad (7)$$

According to matrix inversion lemma [1, pp.124 (3.8.3)], we can derive the $\mathbf{R}_{\mathcal{I}}^{-1}$ as

$$\mathbf{R}_{\mathcal{I}}^{-1} = \frac{L}{\sigma^2} \left\{ \frac{1}{L} \mathbf{I} - \frac{1}{L^2} \mathbf{A} \frac{L}{\sigma^2} \mathbf{S} \left[\frac{L}{\sigma^2} \cdot \boldsymbol{\Psi} \mathbf{S} + \mathbf{I} \right]^{-1} \mathbf{A}^H \right\} \quad (8)$$

where $\boldsymbol{\Psi} \triangleq \mathbf{A}^H \mathbf{A} / L$. Let $\boldsymbol{\psi} \triangleq \mathbf{A}_I^H \mathbf{a}_0 / L$ and $\boldsymbol{\Psi}_I \triangleq \mathbf{A}_I^H \mathbf{A}_I / L$, then $\boldsymbol{\Psi}$ can be written in the following block form

$$\boldsymbol{\Psi} = \begin{bmatrix} 1 & \boldsymbol{\psi}^H \\ \boldsymbol{\psi} & \boldsymbol{\Psi}_I \end{bmatrix}. \quad (9)$$

By (8), we can write $\mathbf{A}^H \mathbf{R}_{\mathcal{I}}^{-1} \mathbf{A}$ as

$$\begin{aligned} \mathbf{A}^H \mathbf{R}_{\mathcal{I}}^{-1} \mathbf{A} &= \frac{L}{\sigma^2} \left\{ \boldsymbol{\Psi} - \frac{L}{\sigma^2} \boldsymbol{\Psi} \mathbf{S} \left[\frac{L}{\sigma^2} \boldsymbol{\Psi} \mathbf{S} + \mathbf{I} \right]^{-1} \boldsymbol{\Psi} \right\} \\ &= \frac{L}{\sigma^2} \left[\frac{L}{\sigma^2} \cdot \boldsymbol{\Psi} \mathbf{S} + \mathbf{I} \right]^{-1} \boldsymbol{\Psi} \end{aligned} \quad (10)$$

In order to further derive the expression for $\mathbf{A}^H \mathbf{R}_{\mathcal{I}}^{-1} \mathbf{A}$, we need to write $[\boldsymbol{\Psi} \cdot L\mathbf{S}/\sigma^2 + \mathbf{I}]^{-1}$ in the following block form

$$\left[\frac{L}{\sigma^2} \cdot \boldsymbol{\Psi} \mathbf{S} + \mathbf{I} \right]^{-1} = \begin{bmatrix} x_{11} & \mathbf{x}_{12} \\ \mathbf{x}_{21} & \mathbf{X}_{22} \end{bmatrix}, \quad (11)$$

where x_{11} , \mathbf{x}_{12} , \mathbf{x}_{21} and \mathbf{X}_{22} are 1×1 , $1 \times D$, $D \times 1$ and $D \times D$ matrix, respectively. In order to derive their expression, we need the following equality [1, pp123]

$$\begin{bmatrix} \mathbf{A} & \mathbf{C} \\ \mathbf{R} & \mathbf{B} \end{bmatrix}^{-1} = \begin{bmatrix} \mathbf{A}^{-1} + \mathbf{A}^{-1} \mathbf{C} \mathbf{S}^{-1} \mathbf{R} \mathbf{A}^{-1} & -\mathbf{A}^{-1} \mathbf{C} \mathbf{S}^{-1} \\ -\mathbf{S}^{-1} \mathbf{R} \mathbf{A}^{-1} & \mathbf{S}^{-1} \end{bmatrix}, \quad (12)$$

where $\mathbf{S} = \mathbf{B} - \mathbf{R} \mathbf{A}^{-1} \mathbf{C}$ is the Schur complement. Substituting (7) and (9) into (11) and using (12) as well as matrix inversion lemma, we can derive

$$x_{11} = (1 - \alpha) \frac{\alpha_1}{\alpha} \quad (13)$$

$$\mathbf{x}_{12} = -(1 - \alpha) \frac{\alpha_1}{\alpha} \frac{L}{\sigma^2} \cdot \boldsymbol{\psi}^H \boldsymbol{\Phi}_{\mathcal{I}} \mathbf{P} \quad (14)$$

$$\mathbf{x}_{21} = -\alpha_1 \cdot \mathbf{P} \boldsymbol{\psi} \quad (15)$$

$$\mathbf{X}_{22} = \mathbf{P} + \alpha_1 \frac{L}{\sigma^2} \cdot \mathbf{P} \boldsymbol{\psi} \boldsymbol{\psi}^H \boldsymbol{\Phi}_{\mathcal{I}} \mathbf{P} \quad (16)$$

where

$$\mathbf{P} \triangleq \left[\frac{L}{\sigma^2} \cdot \boldsymbol{\Psi}_I \boldsymbol{\Phi}_I + \mathbf{I} \right]^{-1} \quad (17)$$

$$\alpha \triangleq \frac{L\sigma_{\mathcal{I}_0}^2}{\sigma^2} \left/ \left[\frac{L\sigma_{\mathcal{I}_0}^2}{\sigma^2} + 1 \right] \right. \quad (18)$$

$$\alpha_1 \triangleq \frac{L\sigma_{\mathcal{I}_0}^2}{\sigma^2} \left/ \left[\frac{L\sigma_{\mathcal{I}_0}^2}{\sigma^2} (1 - \xi) + 1 \right] \right. \quad (19)$$

$$\xi \triangleq \frac{L}{\sigma^2} \cdot \boldsymbol{\psi}^H \boldsymbol{\Phi}_I \mathbf{P} \boldsymbol{\psi}. \quad (20)$$

It is easy to prove that α , α_1 , ξ and \mathbf{P} satisfy the following equalities

$$\alpha_1 = \alpha(1 + \alpha_1\xi)$$

$$\mathbf{P}^H = \mathbf{I} - \frac{L}{\sigma^2} \boldsymbol{\Phi}_I \mathbf{P} \boldsymbol{\Psi}_I$$

which have already been used during the derivation of (13)–(16) and will be used to simplify the expression of $\mathbf{A}^H \mathbf{R}_{\mathcal{I}}^{-1} \mathbf{A}$. Substituting (9), (11), (13)–(16) into (10), after some lengthy but straightforward derivations, we can have

$$\mathbf{A}^H \mathbf{R}_{\mathcal{I}}^{-1} \mathbf{A} = \frac{L}{\sigma^2} \begin{bmatrix} (1-\alpha) \frac{\alpha_1}{\alpha} (1-\xi) & (1-\alpha) \frac{\alpha_1}{\alpha} \boldsymbol{\psi}^H \mathbf{P}^H \\ (1-\alpha) \frac{\alpha_1}{\alpha} \mathbf{P} \boldsymbol{\psi} & \mathbf{P} \boldsymbol{\Psi}_I - \alpha_1 \mathbf{P} \boldsymbol{\psi} \boldsymbol{\psi}^H \mathbf{P}^H \end{bmatrix}. \quad (21)$$

Using (6), (17)–(20), $\text{SNR} = \sigma_{\mathcal{S}_0}^2 / \sigma^2$ and $\beta = N\sigma_{\mathcal{I}_0}^2 / \sigma_{\mathcal{S}_0}^2$ we can finally derive (2)–(4).

The remaining problem is to prove $\xi = \rho_0 - \kappa_0$ and $\kappa \in [0, \rho_0]$, which can also naturally yield $\xi \in [0, \rho_0]$. According to (20) and the definition of $\boldsymbol{\Xi}$, ξ can be written as

$$\begin{aligned} \xi &= \frac{L}{\sigma^2} \boldsymbol{\psi}^H \boldsymbol{\Phi}_I \boldsymbol{\Xi} \boldsymbol{\Psi}_I^{-1} \boldsymbol{\psi} \\ &= \boldsymbol{\psi}^H \boldsymbol{\Xi}^{-1} \boldsymbol{\Xi} \boldsymbol{\Psi}_I^{-1} \boldsymbol{\psi} - \boldsymbol{\psi}^H \boldsymbol{\Psi}_I^{-1} \boldsymbol{\Xi} \boldsymbol{\Psi}_I^{-1} \boldsymbol{\psi} \\ &= \underbrace{\boldsymbol{\psi}^H \boldsymbol{\Psi}_I^{-1} \boldsymbol{\psi}}_{\rho_0} - \underbrace{\boldsymbol{\psi}^H \boldsymbol{\Psi}_I^{-1} \boldsymbol{\Xi} \boldsymbol{\Psi}_I^{-1} \boldsymbol{\psi}}_{\kappa_0}. \end{aligned}$$

Since $\boldsymbol{\Phi}_I$ is positive semi-definite, $\boldsymbol{\Xi}_I^{-1} - \boldsymbol{\Psi}_I^{-1} = \frac{L}{\sigma^2} \boldsymbol{\Phi}_I$ is also positive semi-definite, i.e. $\boldsymbol{\Psi}_I^{-1} \leq \boldsymbol{\Xi}_I^{-1}$.

Then $\boldsymbol{\Psi}_I \geq \boldsymbol{\Xi}_I$, thus

$$\xi = \boldsymbol{\psi}^H \boldsymbol{\Psi}_I^{-1} \left[\boldsymbol{\Psi}_I - \boldsymbol{\Xi} \right] \boldsymbol{\Psi}_I^{-1} \boldsymbol{\psi} \geq 0,$$

which means $\rho_0 \geq \kappa_0 \geq 0$. By the definitions of $\boldsymbol{\psi}$ and $\boldsymbol{\Psi}_I$, we have $\rho_0 = \frac{1}{\|\mathbf{a}_0\|^2} \mathbf{a}_0^H \mathbf{A}_I (\mathbf{A}_I^H \mathbf{A}_I)^{-1} \mathbf{A}_I \mathbf{a}_0$, i.e. the projection power of $\mathbf{a}_0 / \|\mathbf{a}_0\|$ onto $\text{span}\{\mathbf{a}_1, \mathbf{a}_2, \dots, \mathbf{a}_D\}$, which we have assumed to be much smaller than 1 in section II Thus $\rho_0 \ll 1$ and this completes the proof. \square

Lemma 2: Let $\boldsymbol{\psi}_T \triangleq \left[\frac{L\beta}{N}(1-\rho_0)\text{SNR} + 1 \right] \tilde{\boldsymbol{\psi}}_T$ with $\tilde{\boldsymbol{\psi}}_T \triangleq \mathbf{A}_\epsilon \mathbf{R}_T^{-1} \mathbf{a}_0$, then

$$\|\boldsymbol{\psi}_T\| = \sqrt{\frac{L}{\sigma^2} \cdot \frac{\frac{L\beta}{N}(1-\rho_0)\text{SNR} + 1}{\frac{L\beta}{N}(1-\xi)\text{SNR} + 1} \kappa_0} \ll \sqrt{\frac{L}{\sigma^2}} \quad (22)$$

$$\frac{L}{\sigma^2} \boldsymbol{\Phi}_T + \boldsymbol{\Psi}_I^{-1} = \frac{L}{\sigma^2} \mathbf{T}^{-H} \left[\mathbf{I} - \frac{\frac{L\beta}{N}\text{SNR} \cdot \frac{\sigma^2}{L}}{\frac{L\beta}{N}(1-\rho_0)\text{SNR} + 1} \boldsymbol{\psi}_T \boldsymbol{\psi}_T^H \right] \mathbf{T}^{-1} \quad (23)$$

where ρ_0 , ξ and κ_0 are defined in Lemma 1, and are independent of SNR.

Proof: Since $\mathbf{A}_\epsilon = \mathbf{A}_I \mathbf{T}^{-H}$ and $\mathbf{A}_I^H \mathbf{R}_I^{-1} \mathbf{A}_I = \mathbf{T} \mathbf{T}^H$ (c.f. (26) in [2]), (4) is equivalent to

$$\frac{L}{\sigma^2} \left[\boldsymbol{\Xi} - \frac{\frac{L\beta}{N}\text{SNR}}{\frac{L\beta}{N}(1-\xi)\text{SNR} + 1} \boldsymbol{\Xi} \boldsymbol{\Psi}_I^{-1} \boldsymbol{\psi} \boldsymbol{\psi}^H \boldsymbol{\Psi}_I^{-1} \boldsymbol{\Xi} \right] = \mathbf{T} \mathbf{T}^H. \quad (24)$$

Right-multiplying it by $\boldsymbol{\Psi}_I^{-1} \boldsymbol{\psi}$ and using $\rho_0 = \xi + \kappa_0$, we can derive

$$\boldsymbol{\Xi} \boldsymbol{\Psi}_I^{-1} \boldsymbol{\psi} = \frac{\sigma^2}{L} \cdot \frac{\frac{L\beta}{N}(1-\xi)\text{SNR} + 1}{\frac{L\beta}{N}(1-\rho_0)\text{SNR} + 1} \mathbf{T} \mathbf{T}^H \boldsymbol{\Psi}_I^{-1} \boldsymbol{\psi}. \quad (25)$$

Since $\mathbf{A}_\epsilon = \mathbf{A}_I \mathbf{T}^{-H}$, then by (3) and above expression, we have

$$\tilde{\boldsymbol{\psi}}_T = \mathbf{A}_\epsilon^H \mathbf{R}_T^{-1} \mathbf{a}_0 = \frac{L}{\sigma^2} \cdot \frac{1}{\frac{L\beta}{N}(1-\xi)\text{SNR} + 1} \mathbf{T}^{-1} \boldsymbol{\Xi} \boldsymbol{\Psi}_I^{-1} \boldsymbol{\psi} = \frac{1}{\frac{L\beta}{N}(1-\rho_0)\text{SNR} + 1} \mathbf{T}^H \boldsymbol{\Psi}_I^{-1} \boldsymbol{\psi}.$$

Let $\boldsymbol{\psi}_T \triangleq \left[\frac{L\beta}{N}(1-\rho_0)\text{SNR} + 1 \right] \tilde{\boldsymbol{\psi}}_T$, then $\boldsymbol{\psi}_T = \mathbf{T}^H \boldsymbol{\Psi}_I^{-1} \boldsymbol{\psi}$. Using (24), $\rho_0 = \kappa_0 + \xi$ and the definition of κ_0 (Lemma 1), we have

$$\|\boldsymbol{\psi}_T\|^2 = \boldsymbol{\psi}^H \boldsymbol{\Psi}_I^{-1} \mathbf{T} \mathbf{T}^H \boldsymbol{\Psi}_I^{-1} \boldsymbol{\psi} = \frac{L}{\sigma^2} \cdot \frac{\frac{L\beta}{N}(1-\rho_0)\text{SNR} + 1}{\frac{L\beta}{N}(1-\xi)\text{SNR} + 1} \kappa_0.$$

According to Lemma 1, $0 \leq \xi \ll 1$, $0 \leq \rho_0 \ll 1$ and $0 \leq \sqrt{\kappa_0} \leq \sqrt{\rho_0}$. Therefore, $\|\boldsymbol{\psi}_T\| \approx \sqrt{\frac{L}{\sigma^2} \kappa_0} \ll \sqrt{\frac{L}{\sigma^2}}$. We then prove (23). Substituting (25) into (24) and using $\boldsymbol{\psi}_T = \mathbf{T}^H \boldsymbol{\Psi}_I^{-1} \boldsymbol{\psi}$, we can have

$$\boldsymbol{\Xi} = \mathbf{T} \left\{ \frac{\sigma^2}{L} \mathbf{I} + \frac{\left[\frac{L\beta}{N}(1-\xi)\text{SNR} + 1 \right] \frac{L\beta}{N}\text{SNR}}{\left[\frac{L\beta}{N}(1-\rho_0)\text{SNR} + 1 \right]^2} \boldsymbol{\psi}_T \boldsymbol{\psi}_T^H \right\} \mathbf{T}^H.$$

Applying matrix inversion lemma [1] to the above equation and using $\rho_0 = \kappa_0 + \xi$ (Lemma 1), we can finally derive (23). \square

REFERENCES

- [1] C. D. Meyer, *Matrix Analysis and Applied Linear Algebra*. Philadelphia, PA: SIAM, 2000.
- [2] J. Chen, J. Wang, X. Shan, N. Ge, and X. Xia, "Performance Analysis of the Matrix Pair Beamformer with Matrix Mismatch," *submitted to IEEE Transactions on Signal Processing*.